UNIVERSITA' POLITECNICA DELLE MARCHE

FACOLTA' DI MEDICINA E CHIRURGIA

Dottorato di Ricerca XVI CICLO

in

SCIENZE BIOMEDICHE

PANCREATIC DUCTAL ADENOCARCINOMA: BIOMARKER IDENTIFICATION, EXOSOME CHARACTERIZATION, APOPTOSIS AND NECROPTOSIS INDUCTION BY SULFORAPHANE

Relatore:

Dott. Francesco Piva

Dottoranda:

Dr.ssa Giulia Occhipinti

Anno Accademico 2016-2017

Table of content

1. Introduction

1.1 Epidemiology of pancreatic cancers

Cancer is one of the major global public health problems, nevertheless the huge scientific research efforts have achieved, in the last decades, important results in terms of prevention, therapy and reduction of mortality rates. The deadliest cancers are considered those with 5-years relative survival rates below 50% and, according to *Recalcitrant Cancer Research Act,* pancreatic cancer, with 6% of survival, has the lowest percentage followed by lung (16,6%), liver (18%), esophagus (19%), stomach (29%), brain (35%), ovary (44%), and multiple myeloma (45%) [1]. While stomach, lung and breast cancer have shown falls in mortality since the late 1980s, pancreatic cancer mortality has the opposite trends in EU, with a steady rise in women of 3,9% and a stable mortality rate in men in 2016 [2]. Every year worldwide pancreatic cancer deaths are 200000 and it is predicted to be the second cause of cancer death in USA by 2030 [1]. Notably, African-Americans have a 30-50% higher incidence than other ethnic groups in the United States. Indigenous populations seem to be 30% more affected than other populations living in Oceania whereas the lowest rates are recorded in India, Africa and Southeast Asia. In this geographical variation, the quality of clinical diagnoses and the differential access to health care have to be taken into account because these evaluations could be altered by under diagnosis [3].

1.2 Risk factors

Pancreatic cancer incidence rate could be attenuated modifying some aspects of the life style. Among preventable factors, tobacco smoking is the most common agent, and it increases threefold the risk of developing pancreatic cancer [4]. It has been estimated that 25% of pancreatic cancers are attributable to cigarette smoking. Interestingly, the sequencing of pancreatic cancer genome has revealed that smoker patients have more somatic mutations than never-smoker patients. Other life habits connected with the frequency of this disease are low physical activity and some dietary factors like high consumption of saturated fats, red and processed meat and low intake of vegetables and fruits. Moreover, it has been observed that heavy alcohol consumption is correlated with the tumour incidence, while moderate alcohol intake does not induce an increased risk [4]. Additionally, some pathological states can

contribute to the neoplasm onset. Obesity is positively associated with pancreatic cancer, specifically, high body-mass index and centralized fat distribution may increase the risk [5]. Diabetes mellitus is not only a consequence of early-stage pancreatic cancer but it is also a risk factor. Diabetic patients have a 30% possibility of developing a tumour for more than 20 years after diagnosis [6].

Some hereditary conditions can also increase the risk of developing the disease. Several studies have demonstrated that 10% of patients have a family history of ductal adenocarcinoma of the pancreas, but the majority of the genetic basis remains unknown. Some germline genetic syndromes have been associated with an increased risk of developing this neoplasia. Inherited mutations in onco-suppressor genes BRCA2 and BRCA1 are associated with elevated risk of breast and ovarian cancer. While BRCA2 mutations account for familial pancreatic cancer, the role of mutated BRCA1 remains uncertain. Germline mutations in the *p16*/CDKN2A causes familial atypical multiple mole melanoma syndrome with a high lifetime risk of melanoma, as well as an increased risk of pancreatic cancer. Patients with Peutz-Jeghers syndrome, caused by germline mutations in STK11, have been shown to have an 11-32% lifetime risk of pancreatic cancer in addition to hamartomatous polyps in the gastrointestinal tract. Hereditary pancreatitis is a rare form of pancreatitis caused by mutations in PRSS1 and SPINK1. Patients with these alterations have a 30-40% possibility of developing cancer. Individuals with Lynch Syndrome, a disease caused by germline mutations in genes encoding DNA mismatch repair proteins, are characterized by early onset colon cancer and have an elevated risk of vary cancer types, among which is pancreatic cancer [4, 7].

1.3 Pancreatic tumours and PDAC pathogenesis

Pancreatic ductal adenocarcinoma (PDAC) is the most common and aggressive malignancy arising from the pancreas. Less frequent pancreatic neoplasms are neuroendocrine tumours, solid-pseudopapillary neoplasms, pancreatoblastomas, acinar carcinomas and colloid carcinomas.

Pancreatic neuroendocrine tumours (PanNETs) are the second most common neoplasm, representing 1-5% of all pancreatic tumours, with a mortality rate of 60%. They could arise as part of hereditary syndromes: multiple endocrine neoplasia type 1

(MEN-1), von Hippel-Lindau syndrome (VHL) and tuberous sclerosis complex (TSC). PanNETs are classified into functioning tumours which give early symptoms caused by excessive hormone production and non-functioning tumours that manifest only when they are large [8]. Solid-pseudopapillary neoplasms represent 1-2% of primary pancreatic tumours. This type appears as a heterogeneous low-grade malignant tumour with solid components and cysts and it is frequent in young women. Pancreatoblastoma accounts for 0,2% of all pancreatic neoplasms and it mostly occurs in children. At presentation, it is a large mass with aggressive behaviour and metastasis. Pancreatic ductal adenocarcinoma occurs in 90% of cases and has a remarkably poor prognosis. PDAC incidence is 50% higher in men than in women and old age is also a significant factor with most cases occurring in patients between 60 and 80 years. Pancreatic adenocarinomas are located in the head of the pancreas in 60-70% of patients, 10–20% in the body, and 5–10% in the tail. Principal marks, that appear too late in the disease course, are abdominal pain, weight loss and jaundice [9]. These tumours are solid and firm, derived from neoplastic cells which infiltrated into tissues forming glands and spread far from the primary tumour. Invasive cancer colonizes nerves, perineural and lymphatic spaces until it spreads to the liver. One of its important histologic traits is the intense desmoplastic reaction, which impedes biopsy to reach neoplastic glands and constitutes an obstruction for chemotherapeutic agents [3, 4]. Lack of early symptoms, absence of sensitive and specific biomarkers and the challenging identification of early-stage tumours are the principal reasons of a late diagnosis. Moreover, PDAC is characterized by high aggressiveness that leads to exclude surgical resection in most patients due to vascular invasion and early spread of metastasis. Traditional treatments like chemotherapy and radiotherapy are not effective since pancreatic tumour cells have resistance to the majority of anti-cancer agents [3].

Pancreatic ductal adenocarcinoma originated from non-invasive lesions. In 82% of pancreas with cancer, intraductal non-invasive proliferations called pancreatic intraepithelial neoplasia (PanIN) are observed. Timely detection of these precursor lesions may be crucial for an early diagnosis but so far their detection is challenging due to the lack of symptoms, specific biomarkers and mainly because of their microscopic size, which makes them not easily detectable by Magnetic Resonance

Imagery (MRI) or by Computed Tomography (CT). PanINs are classified into three grades depending on the cytological atypia. Low grade PanINs are found in 16-80% of normal pancreas without neoplasia while high grade PanINs are related to adenocarcinoma [10]. Less frequently, pancreatic cancer derives from macroscopic cystic precursors: intra-ductal papillary mucinous neoplasm (IPMN) and mucinous cystic neoplasm (MCN). IPMNs involve the larger pancreatic ducts, are larger than 1 cm in size and approximately a third of them are associated to a higher risk of developing invasive adenocarcinoma. MCNs occur particularly in women, arise in the body and the tail of pancreas, and do not involve the ductal system [7].

1.4 Genetic mutations

Cancer is a genetic disease caused not only by inherited mutations but also by somatic mutations involving tumour suppressor genes and oncogenes. The sequencing of infiltrating pancreatic ductal adenocarcinoma revealed that there are four major driver genes, KRAS, p16/CDKN2A, TP53 and SMAD4, somatically mutated in more than 50% of the cases. Precursor lesion analyses have sketched out the timing of the genetic alterations in pancreatic tumourigenesis. KRAS and CDKN2A mutations occur in low-grade PanINs, suggesting that they are the earliest alterations in pancreatic tumourigenesis. KRAS is an oncogene that encodes a small GTPase protein involved in the activation of MAP Kinase and/or the PI3K pathways that increase mitogenic activity. Its mutational activation results in the downstream activation of effector proteins that sustain proliferation, cell migration and metastasis. CDKN2A is a tumour suppressor gene inactivated in 95% of PDAC. Its mutation is associated to unlimited cell growth caused by the loss of function of its protein product, p16, an important cell cycle regulator. TP53 and SMAD4 mutations take place at an advanced stage of the carcinoma, suggesting that they are late events. The tumour suppressor TP53 codes for p53 protein, which responds to several cellular stresses inducing growth arrest and cell death. Loss of p53 function is observed in 75% of pancreatic cancers. The protein product of SMAD4 gene, Smad4, plays an important role in the TGFβ pathway and in transcription of cell cycle inhibitory factors like p21. Thereby, SMAD4 inactivation, in about 50% of cases, is linked to poor prognosis and metastatic disease [4, 7].

1.5 Microenviroment

Pancreatic ductal adenocarcinoma is different from other solid cancers because of the desmoplastic reaction, an abundant and dense collagenous stroma, which envelops malignant cells. This stroma contains extracellular matrix (ECM) proteins, such as collagens, fibronectin and laminin, non-collagenous proteins (glycoproteins, proteoglycans and glycosaminoglycans), as well as growth factors, osteopontin, periostin and serine protein acidic and rich in cysteine that may mediate the interaction of cancer cells and ECM [3]. Cellular component of desmoplasia consists of cancer-associated fibroblasts (CAFs), which produce the collagenous matrix and immune cells that could regulate the cancer growth. For these reasons, there has been growing interest in the role of desmoplasia in malignant and aggressive behaviour of pancreatic cancer and its resistance to treatment. Pancreatic stellate cells (PaSCs) are the principal cellular source of CAFs in pancreatic cancer. They are present in the exocrine pancreas in a normal quiescent state but are transformed in an activated state during the pathogenesis. Activated PaSCs have high proliferation rate and start to produce ECM proteins and the other components of desmoplasia. Several studies have demonstrated that this activated state is maintained not only by autocrine but also paracrine mechanisms with inflammatory and cancer cells. This relationship results in an increased tumour growth and metastasis development [11]. Interaction of pancreatic stellate cells with cancer cells and other stromal cancer cells promotes cancer progression. They are probably implicated in the formation of new blood vessels (angiogenesis) through the production of the proangiogenic factors: vascular endothelial growth factor (VEGF), platelet-derived growth factor (PDGF) and hepatocyte growth factor (HGF). These factors are found to be up-regulated in tumour tissue and are associated with poor prognosis [12]. Furthermore PaCSs promote stem-cell like phenotype conferring chemo-resistance upon pancreatic cancer cells [13]. These cells are also able to travel from the primary tumour, surviving in the circulation, and seed metastatic niches to distant organs [14]. The desmoplastic stroma is composed also by different type of inflammatory cells: macrophages, T cells and neutrophilic granulocytes, that contribute mostly to the tumour progression. For example, CD4+ regulatory T cells have the decisive role in keeping away the host immune system, and M2 macrophages synthesize cytokines and chemokines involved

in tumour angiogenesis and metastasis. Factors implicated in the antitumour immunity suppression, for example PD-L1, are clinically important because they could be targets for new immunotherapeutic approaches [3, 15].

Metastasis formation needs a supportive environment that is established prior to the arrival of carcinoma cells, the so-called pre-metastatic niche. This environment is the result of numerous signalling factors from primary tumour to distant tissue that lead to the formation of metastasis [16]. Exosomes, nanovesicles secreted from cells by exocytosis, play an important role in this process. It has been demonstrated that pre-mestatic niches in the liver of naive mice are caused by PDAC-derived exosomes formation. Exosome uptake by hepatic cells induced TGFβ secretion and production of fibrotic microenvironment by hepatic stellate cells. In particular, it seems that the exosomal macrophage migration inhibitory factor (MIF) prepares the liver for metastasis since it was found highly expressed in exosomes derived from patients with late-stage cancer [17]. The role of exosomes in cancer is described in detail in the chapter 3.

1.6 Biomarkers

The importance of finding reliable biomarkers arises from the difficulty to detect the early stage of PDAC but also for evaluation of treatments or post-resection follow-up. Liquid biopsy is an alternative to surgical biopsies that allows detection of circulating tumour cells and so cancer at an early stage. It is a promising approach for the evaluation of new cancer markers in a non-invasive and easy way, generally through blood samples, instead of tumour tissue samples that are often difficult and time-consuming to obtain and to analyse. Moreover, liquid biopsy can be repeated several times during the therapy period without pain and risk for the patients, allowing the monitoring of tumour relapses or the occurrence of resistance mutations [18]. Among serum markers, carbohydrate antigen 19-9 (CA19-9) is the most widely studied. However, CA19-9 lacks sensitivity and specificity since the protein levels are often normal in the early stages of the disease or falsely high in individuals with other pathological conditions. These factors make it an inaccurate marker but it is nonetheless used to control disease progression, recurrence after surgery detection and therapy response. Carcinoembryonic antigen (CEA) could also be a diagnostic tool

but with low reliability [19]. Instead, it has been reported that CA19-9 and CEA combination or CA19-9, CA125 and laminin γC (LAMC2), increase specificity compared with the markers alone [7]. Another marker that could be detected non-invasively in the circulation is tumour DNA that can be extracted from circulating tumour cells (CTCs), intact and viable cells that are distinguished and isolated from the normal blood cells. Disadvantage of circulating tumour cells is that they are present only in some patients with advanced neoplasia. On the contrary, circulating tumour DNA (ctDNA), not associated with cells, has been found in blood samples in patients with localized disease. Using digital polymerase chain reaction–based technologies (dPCR) it is possible to evaluate somatic mutations of circulating DNA [18]. In a recent study, mutated KRAS has been detected from ctDNA of 43% of the patients at the time of diagnosis, indicating that this approach is a highly specific tool for early diagnosis [20].

Body fluids are also enriched in exosomes, extra-cellular vesicles participating in intercellular communication. They are a rich source of information since they are constituted by specific microRNAs, proteins, lipids and other nucleic acids, and thus are generating a big interest as tumour biomarkers. In particular, they bring on their external surface specific proteins that allow distinguishing exosomes derived from different subpopulations of pancreatic cancer cells. It is well known that tumour-derived exosomes express the same markers of cancer-initiated cells, which are implicated in metastasis formation, drug resistance and cancer recurrence. A recent work has demonstrated that circulating exosomes, from pancreatic cancer patients and genetically engineered mutant mice models, showed the proteoglycan glypican-1 on the membrane. Glypican-1 positive exosomes carry the KRAS mutation, allowing the distinction between healthy individuals and patients with early or late pancreatic cancer [21].

During my PhD, I analysed plasma samples of PDAC patients, using exosome markers, with the aim of finding a correlation between different kinds of exosomes and patient clinical data that might be informative as prognostic and diagnostic tools (chapter 3).

MicroRNAs enclosed in these nano-vesicles are considered potential biomarkers since they are specifically and differently expressed depending on the disease features: tumour growth, drug resistance or metastasis progression. Therefore, their evaluation in biofluids could be informative for the early detection of pancreatic cancer. To

measure exosomal miRNAs accurately is tricky and great care should be paid in all the experimental procedures, starting from samples handling, exosome isolation and miRNA extraction, in order to avoid contaminations that can affect the results. In Occhipinti et al. (2016) I have dealt with the problem of the choice of an RNA that can be used as normalizer for the quantification of miRNAs expression levels in exosomes. To make the measures from different samples by reverse transcription quantitative real-time polymerase chain reaction (RT-qPCR) comparable, it is important to normalize selecting an endogenous control permanently expressed among all the samples examined. In that review, I discussed the studies where the exosomal miRNA profiling was assessed in human biofluids highlighting the specific RNA used as normalizer [22].

Microarray analysis of gene expression profiles have revealed that hundreds of genes resulted to be differently expressed in pancreatic tumour tissues compared to normal tissues, and that therefore may serve as biomarkers. This method has allowed the outlining of a list of genes that are inversely related to PDAC patient survival: keratin 7, laminin gamma 2, stratifin, platelet phosphofructokinase, annexin A2, MAP4K4 and OACT2 (MBOAT2) [23]. Gene expression analysis has also permitted to find that high levels of PIK3R1 expression are correlated with improved survival contrary to SRC [24]. In another study, microarray gene-expression data from tumour and adjacent non-tumour tissues of PDAC patients revealed that DPEP1 could be a prognostic relevant gene in PDAC, since its low expression is related to poor prognosis. Further validation on pancreatic cell lines showed that over-expression of DPEP1, suppressed tumour cells invasiveness increasing sensitivity to Gemcitabine [25].

It is possible to identify new candidate biomarkers by processing expression data with bioinformatic tools that take account of correlation among genes. With this aim, the weighted gene co-expression network analysis (WGCNA) algorithm has been applied, as described in chapter 4. This approach has allowed the detection of key genes and miRNAs involved in tumourigenesis of PDAC [26, 27].

1.7 Treatment

Surgery, chemotherapy, radiotherapy and palliative care are the treatment choices selected according to the stage of pancreatic cancer.

Surgical resection is the option that prolongs life in comparison to the other treatments with 5-year survival rates of 20%. However only 10-20% of patients have resectable diseases, and 80% of these cases undergo a relapse despite tumour resection and adjuvant therapy. Pancreatic cancers without metastases can be classified as resectable, borderline resectable and locally advanced, depending on the degree of local extension that could involve mesenteric or portal vein, gastroduodenal and hepatic artery or could form a tumour abutment of the superior mesenteric artery. Traditionally, surgery is performed by an open procedure, but at the present, the use of laparoscopic or robotically assisted resections is increasing. Tumour surgery that includes venous resection is usually a low risk procedure whereas arterial resection increases the mortality rate. However, frequently, recurrence of PDAC is reported after surgical operations, and the median survival could be similar to that of inoperable patients. The main causes are occult primary metastases and microscopically incomplete resections. For these reasons, specialized surgeons and pathologists, as well as an accurate selection of patients for resection, are crucial. Parameters to consider in selecting patients are the absence of comorbidities, such as cardiac disease, and age, which should be not higher than 75 years, otherwise the patient could be further debilitated. It is also important to consider the tendency of metastatic spread and tumour aggressiveness. Even though there are not validated biomarkers, indicators of aggressive tumour are significantly high serum levels of CA19-9 and SMAD4 alteration. Patients with these traits are unlikely to benefit from resection and therapy compared to patients with low CA19-9 levels and wild-type SMAD4. Surgery alone is anyway associated to poor survival so adjuvant therapy, with gemcitabine or 5-fluorouracil (5-FU) and leucovorin, is the standard care started 1-2 months after resection. Several studies have demonstrated that 6 months treatments improved significantly survival patients compare with no adjuvant treatment after surgery or with chemotherapy alone [3, 4, 7].

For patients with metastatic and unresectable PDAC the survival rate is 5-9 months, so the main purposes of treatments are pain alleviation and improved survival. Gemcitabine is the standard treatment for elderly patients for its favourable toxicity profile. Agent combinations such as FOLFIRINOX (folinic acid, 5-FU, irinotecan and oxaliplatin) or gemcitabine with nab-paclitaxel result in a longer survival and in an

improved quality of life but are more toxic than gemcitabine monotherapy. For this reason, their use is limited only to patients in a good health status. About 50% of patients in good performance status receive second-line chemotherapy after disease progression which might be useful for their benefit. Effective second-line treatment could be combinations like 5-FU with oxaliplatin, FOLFIRI (5-FU, irinotecan and leucovirin) or gemcitabine monotherapy [28].

However, current standard therapies have provided scarce survival advantage highlighting the urgent need to identify new treatment strategies and agents. Among new therapeutic strategies, drugs targeting vital pathways for pancreatic cancer stem cells (CSCs) are promising. Such cells play a role in initiation of new tumour foci, disease relapse and chemotherapeutic-resistance because of their ability to self-renew. The pathways targeted for this purpose are WNT, Notch and Hedgehog but until now completed trials have shown negative results and CSCs continue to confer a shorter survival [29]. Recent studies have focused on the anti-cancer properties of plant-derived compounds that can have effects not only on cell cycle regulation and apoptotic pathways but also on non-apoptotic pathways such as autophagy and programmed necrosis (necroptosis) [30, 31]. In the last part of my thesis, as described in chapter 5, I investigated the question whether Sulforaphane eliminates pancreatic cancer cells by inducing apoptosis and/or necroptosis. Sulforaphane is a plant-derived agent, which has shown health-promoting and anti-cancer properties [32].

2. Aim of the thesis

My thesis is focused on the study of pancreatic ductal adenocarcinoma using different approaches: i) exosome characterization and quantification in clinical samples in order to evaluate if exosome levels correlate with progression of the disease; ii) identification of potential diagnostic and prognostic biomarkers through the application of the weighted gene co-expression network analysis (WGCNA) tool; iii) investigation on programmed cell-death pathways induced by the broccoli-derived isothiocyanate sulforaphane in pancreatic cancer cell lines.

To reach the first goal, a convenient enzyme linked immunosorbent assay (ELISA) was developed for the detection of exosomes in plasma samples from PDAC patients. This study was funded by an AIRC grant and patient samples were procured by Medical Oncology Unit of Ospedali Riuniti Ancona.

In the second part of my thesis, WGCNA tool was applied, for the first time, to PDAC microarray-based gene and microRNA expression datasets, respectively from normal and PDAC tissues samples and from serum samples of PDAC and healthy individuals.

I conducted the last part of my PhD thesis in the Department of Molecular OncoSurgery at the University Hospital of Surgery in Heidelberg (Germany) where I worked as visiting PhD student supervised by Prof. Ingrid Herr.

3. Exosome characterization in pancreatic cancer patients

3.1 Introduction

3.1.1 Exosomes

Intercellular communication is a vital system for multicellular organisms and it is exerted by several different mechanisms. In addition to direct contact between cells or active and passive transfer of secreted molecules, another communication system, which has gained a large interest, is constituted by vesicular transport. Under physiological and pathological conditions, cells can secrete different types of vesicles, depending on their cellular origin, divided mostly in two classes: microvesicles and exosomes that are differentiated for their biogenesis, size and composition. Microvesicles derive from the outward budding and fission processes of the plasma membrane and their size range from 200 nm to more than 1 μm in diameter. Exosomes are smaller than microvesicles, ranging between 30-120 nm. They originate from endocytic invagination of the plasma membrane and then are progressively released into extracellular space [33, 34]. These nanovesicles were identified for the first time in the 1980s when, during studies about reticulocyte maturation was observed a different mode of vesicles excretion. Later, in 1987, the term “exosomes” was proposed, indicating the endosomal origin of these vesicles and it was demonstrated that they contained active enzymes [35]. In 2007, description of miRNA and mRNA transported by exosomes led to an increasing interest in discovering their functions [36, 37]. Exosomes have been isolated from almost all body fluids: serum, plasma, breast milk, urine, malignant ascites, amniotic fluid and saliva, leading researchers to consider them as novel tools for early diagnosis [38-40]. Exosomal lipid layer protects miRNAs from endogenous RNases even in extreme conditions such as in faeces [41] or in a simulated gastric and pancreatic digestion [42]. These findings suggest that exosomal miRNAs can exert their influence to distant target cells since their integrity is preserved in body fluids and that genetic material may be transferred via exosomes in breast milk to the infants [42, 43].

3.1.2 Biogenesis, secretion and uptake

The process of exosome biogenesis begins with the endocytosis of the plasma membrane that takes place after the ubiquitination of membrane receptors. This process is followed by the formation of early endosomes and, successively, of the multivesicular bodies (MVBs). They generate, through internal budding, intraluminal vesicles (ILVs) that are eventually released in the extracellular space as exosomes. MVBs can also be addressed to the lysosomes for degradation or to the trans-Golgi network for recycling. Endosomal Sorting Complex Required for Transport (ESCRT) machinery intervenes in ILVs formation and exosomal content sorting. ESCRT is made of four main protein complexes involved in ubiquitin-dependent cargo assemblage, bud formation and vesicle scission [33]. Exosomal content can be determinated by other mechanisms ESCRT-independent involving lipids, tetraspanins or heat shock proteins that serve as receptor for enclosing specific cytoplasm components such as proteins and microRNAs. Exosomes are secreted from the sender cell through exocytosis. In this mechanism Rab GTPase plays the role of moving the late endosome towards a site of plasma membrane while SNAREs proteins promote the fusion of MVBs membranes with the plasma membrane. Intracellular Ca+ levels and extracellular/intracellular pH gradients also affect exosome release. It has been shown that low pH in the microenvironment leads to an increased exosome secretion and uptake [33, 36, 44]. Exosomes can transfer material to recipient cells in different ways. The receptor-mediated uptake can occur via some phospholipids and proteins on the exosomal membrane that act as receptors to bind the cell membrane. Endocytosis by phagocytosis is another way to incorporate exosomes that are actively transported by the cytoskeleton. Finally, the uptake can occur through membrane fusion facilitated by low pH [33].

3.1.3 Exosomes composition

Lipids. Lipid composition of exosomes depends of cellular origin but generally consists of cholesterol, sphingomyelin, ceramide, phosphatidylcholine (PC), phosphatidylserine (PS), phosphatidylethanolamine (PE), phosphatidylinositol (PI). Some exosomal lipids, such as sphingomyelin, cholesterol, PS, PC and PI, are present in higher quantities compared to parental cells conferring an elevated membrane rigidity [45]. Exosomes are also composed of lipid rafts associated with proteins such as Flotillin-1 and

glycosylphosphatidylinositol-anchored proteins [46]. Lipids also have a functional role in exosomes. Lysobisphosphatidic acid (LBPA) may help the formation of the intraluminal vesicles in MVBs and participates in exosomes segregation [47]. Moreover, these vesicles contain bioactive lipids, such as prostaglandins and leukotrienes, which are delivered to target cells and enzymes involved in their metabolism suggesting that exosomes produce autonomously such lipids [48, 49].

Proteins. Exosomes, depending on their endosomal origin, contain numerous membrane transport and fusion proteins: Rab, GTPase, SNAREs, annexins and flotillins. The exosome membrane is enriched in tetraspanins, a protein family constitute of four transmembrane domains. They are implicated in biological process such as signalling and protein trafficking, cell motility, adhesion and membrane fusion. The first identified in B cell-derived exosomes were CD63, CD81, CD82, CD53 and CD37 while CD9 was identified for the first time in exosomes secreted from dendritic cells. Subsequent studies have demonstrated that tetraspanins are present also in exosomes derived from other cells [46, 50]. Tetraspanins are involved also in selection and incorporation of specific material inside exosomes, for example, CD9 loads the metalloproteinase CD10 [51]. Other typical proteins are the heat shock proteins (Hsp70 and Hsp90), Alix and TSG101 which are involved in MVB biogenesis. tetraspanins, Alix, flotillin, TSG101, and Rab5b are the most routinely used as markers for exosome identification in antibody-based techniques such as western blot and ELISA [52]. Exosomes incorporate also proteins implicated in cell signalling pathway. It has been demonstrated that exosomes secreted from *Drosophila* and human cells bear on their membrane active Wnt proteins that induce the related signalling pathways in target cells. The study suggests also the evolutionary conserved role of exosomes in Wnt transportation [53]. Notch ligand Delta-like 4 (Dll4) is also included in exosomes implicating the inhibition of Notch signalling [54]. Tumour-derived exosomes are enriched of all cancer stem cells markers. For examples MART1 has been found in melanoma exosome, EpCAM is included in exosomes derived from epithelial cells and glioma exosomes contain EGFRVIII [55].

Nucleic acids. An important discovery, which has made possible to confirm the regulative role of exosomes in intercellular communication, was the demonstration that they enclose nucleic acids. Microarray analysis allowed Valadi and colleagues

(2007) to describe for the first time about 1300 genes in exosomes from mouse and human mast cell lines. Then they showed that mRNAs and microRNAs (miRNAs) contained in exosomes can be functional in target cells since in these cells new proteins were found [37]. After this finding, numerous other studies described the presence of small RNAs (mRNA and microRNA) and ribosomal 18S and 28S RNAs in exosomes purified from other human cells [56]. MicroRNAs are small non-coding RNAs, which regulate numerous developmental and physiological processes by targeting mRNAs, causing their degradation and downregulation of protein expression. miRNAs have attracted a greater interest among molecules contained in exosomes due to their regulatory roles in gene expression. It is well known that pre-miRNAs in the nucleus, after Drosha processing, are exported into the cytoplasm by Exportin-5 (Exp5) where they are digested by the cytoplasmic ribonuclease III-like endonucleases Dicer [57]. Likewise, the sorting of mature miRNAs in exosomes is specifically regulated. It was found that the 3' portion of miRNA sequence presents some sorting signals. For example, GGAG motif is recognized by sumoylated heterogeneous nuclear ribonucleoproteins A2B1 (hnRPNsA2B1) which import specific miRNAs in exosomes. miRNAs with 3'-end uridylated are preferably distributed inside B cells derived-exosome differently from the B cells where adelylated endogenous miRNAs are found. The neural sphingomyelinase 2 (nSMase2) was demonstrated to be involved in exosomal microRNA secretion in cancer cells. The human AGO2 protein mediates the interaction among mRNA and microRNA, but recently it has been found a potential involvement of this protein in exosomal miRNA sorting. These evidences suggest that miRNAs are not randomly incorporated in exosomes. Indeed, miR-451 is highly expressed in HMC-1 and HEK293T cell lines or in primary T lymphocytes while miR-320 family members are widely included in exosomes from normal and tumour tissue. The expression level of miR-21 is lower in exosomes isolated in serum from healthy donors than in glioblastoma patients, and let-7 family are abundant in gastric cancer-derived exosomes but not in other cancer cell lines. Interestingly, exogenous miRNAs from viruses can also enter exosomes in order to use them as a vector towards non-infected cells [58].

Several studies showed that short DNA sequences are in exosomes too. Mitochondrial DNA was found in exosomes from myoblasts [59] and single-strand DNA was isolated

in microvesicles from glioma cell line [60]. Kahlert et al.(2014) identified for the first time the presence of double-stranded genomic DNA in exosomes from pancreatic cancer cell lines and in serum patients [61]. Gradually, other studies have confirmed the presence of DNA in exosomes from cancer cell lines and in plasma samples from cancer patients, as well as from seminal fluid, blood and urine [62].

3.1.4 Roles of exosomes in cancer

Tumour cells have the capacity to create a microenvironment where normal cells are recruited in order to support tumour cells survival and propagation. Tumour-derived exosomes play an important role in the communication between cancer cells and tumour environment. The extracellular matrix (ECM) is an important component of the primary tumour as evidenced by several studies that suggested that stromal cells are stimulated by tumour-derived exosomes to secrete biological factors such as the oncogenic receptor EGFRvIII20, Matrix Metalloproteinase 9, Vascular Endothelial Growth Factor, Interleukin 8 that promote tumour metastasis. In addition, exosomes could induce ECM degradation with important consequences on tumour cell motility, adhesion and invasiveness [63]. Moreover, they support the metabolic demands of colonizing tumour cells through the promotion of angiogenesis. It has been found that endothelial derived exosomes included and transferred to other endothelial cells Dll4 which inhibited Notch signalling stimulating the formation of capillary-like structures [64]. Exosomes from LAMA84 chronic myeloid leukaemia (CML) cells secreted IL-8 mediating activation of VCAM-1 and so inducing vascular differentiation [65]. Hypoxia is a specific trait of tumour microenvironment and tumour-derived exosomes can mediate intercellular signalling in this condition too. It has been demonstrated that exosomes from glioblastoma multiforme (GBM) cells, which grow under hypoxic condition, significantly stimulated angiogenesis compared with those produced in normoxic envirorment [66]. Exosomes also play an important role in the development of cancer drug resistance, which is caused by several factors, such as: the epigenetic suppression of tumour suppressor proteins activated by miRNAs, the role of desmoplastic reaction as drugs barrier, the presence of stem-like cells that are highly resistant [43].

3.1.5 Exosome isolation and quantification techniques

Techniques that allow exosomes isolation from different body fluids or cell culture supernatants are based on vesicle physical properties, such as size and density. The choice among these techniques usually depends on sample volume and downstream applications. Differential ultracentrifugation is considered the standard method for the isolation of these nanovesicles and it has been the most commonly used for several years. This method uses successive centrifugations at increased speeds in order to eliminate dead cells and large cell debris. Pellets consisting of smaller particles are gradually discarded until the final supernatant, which is centrifuged at the high speed of 100000 g for several hours. The resulting pellet consists of exosomes [67]. However, extravesicular protein complexes or lipoproteins can contaminate the exosome pellet because they sediment at the same speed. Density gradient ultracentrifugation separates particles depending on their density by using a sucrose solution at different concentrations. The latter method can be used as a continuation of ultracentrifugation protocol with the purpose of separating exosomes from non-vesicles contamination, obtaining a purer exosome fraction. Disadvantages of both methods are the time necessary for the overnight spins and the need for extensive sample handling. Because of low-volume and large numbers of clinical samples, ultracentrifugation is not appropriate for routine clinical practice [67, 68]. An alternative method consists in commercial kits such as ExoQuick™ (System BioScience) or Exosome Isolation Reagent (Life Technologies) which precipitate exosomes using water to exclude polymers. They are easy to use and do not require ultracentrifuging but only low speed centrifugation to obtain the exosome pellet. Nevertheless, exosome yields are variable and the purity can be affected by protein association [69].

When exosomes are purified, their quantification can be accomplished by different approaches. Nanoparticle tracking analysis (NTA) examines the light scattering produced by particle movement under Brownian motion in liquid suspension. A drawback of this method is that it cannot discriminate between exosomes or small debris of the same size range because it does not identify the composition (proteins, lipids, etc.) of the particles [22]. Flow cytometry is an effective method for the quantitative and qualitative analysis of cells and it could be adopted for extracellular vesicles even though with several difficulties due to their small size and low refractive

index. The most used protocol for flow cytometry consists in labelling isolated exosomes with lipophilic dye PKH67 and antibodies, but it is not easy to calibrate the machine and necessitates an experienced operator [70]. Exosomes can also be bound to beads coupled with antibodies that guarantee a large surface and high specificity but the detection is dependent on the antigen availability [70].

Enzyme linked immunoassay (ELISA) is a commonly used method for protein detection and quantification. It is based on highly specific non-covalent antigen-antibody binding in samples containing myriads of different proteins. There are different formats of this assay. The key step is the antigen immobilization that can be carried out by the direct adsorption to the plate or through the capture antibody that has been attached to the plate. Then, the antigen can be detected by labelled primary antibodies (direct ELISA) or by labelled secondary antibodies, which specifically recognize the primary one (indirect ELISA). Another format is called ELISA sandwich because the antigen is bound between the capture antibody and the detection antibody. The antibodies can be labelled with an enzyme which catalyses the conversion of chromogenic substrates into coloured product (colorimetric ELISA), becomes fluorescent (immunofluorescence assay) or chemiluminescent (chemiluminescence analysis). Immunoassays seem to have more advantages for exosomes isolation compared to the other mentioned precipitation based techniques. Indeed, this method results in an elevated efficiency of recovered exosomes from complex matrices like body fluids and it is much more specific due to the antibodies that can identify one of the different proteins expressed on exosome surfaces. ELISA assay has been demonstrated to be a robust method for the detection and quantification of disease-derived exosomes in human biological samples and tumour models [69, 71].

In this work, I have first optimized an ELISA protocol in order to isolate the exosome fraction from human plasma samples in order to maximise the signal of plasma samples and reduce the background noise. Specifically, I have evaluated the most suitable blocking agent, washing solution and antibody dilution buffer.

The obtained protocol was used for the project funded by an AIRC (Associazione Italiana per la Ricerca sul Cancro) grant and in collaboration with the Medical Oncology Unit of Ospedali Riuniti Ancona. Blood samples were collected from PDAC patients

before and after chemotherapy treatment in order to measure, through our customized protocol, levels of different exosome populations by using primary antibodies that bind both ubiquitous (CD9, CD81, Alix) and tumour markers on the exosome surface. Pointedly, we measured those proteins which have been already found in tumour exosomes of pancreatic cancer such as CD44v6, Tspan8, EpCAM [72] or other pancreatic cancer initiating cells (CICs) markers: CD24, CXCR4, Integrins α6 and β4, CD133 [73, 74] that are transferred on exosome membranes. This could allow the identification of a potential correlation between the levels of exosomal biomarkers and treatment efficacy.

3.2 Materials and Methods

3.2.1 Patients

Sixteen patients were selected for the enrolment in the study by the Medical Oncology Unit of Ancona. One patient, *P7,* was enrolled after having received radical surgery for PDAC with no signs of disease relapse at the time of admission into the study. The remaining 15 were patients with metastatic/locally advanced pancreatic cancer that were treated with palliative chemotherapy. Specifically, 13 patients (*P1, P4, P5, P6, P8, P9, P10, P11, P12, P13, P14, P15*, *P16*) had metastatic disease upon study entry whereas the remaining two (*P2* and *P3* patients) had locally advanced, and so, unresectable pancreatic cancer. Ten patients received as first-line chemotherapy Gemcitabine in combination with Nab-Paclitaxel whereas three patients received FOLFIRINOX. The remaining two patients received Gemcitabine palliative chemotherapy alone.

Disease Status	**Patients**	**Time Sampling (Months)**					
metastatic	*P1*	0			3		
	P4	0			3		
	P5	0			3		
	P6	0		2	3	6	
	P8	0	1	2	3	6	8
	P9	0	1				
	P10	0	1	2	3	6	
	P11	0	1			6	
	P12	0	1		3		
	P13	0	1		3		
	P14	0	1		3		
	P15	0	1				
	P16	0	1		3		
locally advanced	*P2*	0			3		
	P3	0			3		
resectable tumour	*P7*	0	1	2	3		

Table 1 List of enrolled patients with their disease status at the time of admission into the study and blood sampling time.

3.2.2 Blood samples

Blood samples were taken before chemotherapy treatment (T_0) and, when possible, after one, two and three months (T_1, T_2, T_3). Only in a few cases blood samples were taken six (T_4) and eight (T_5) months after the treatment (Tab. 1). Plasma was separated from blood cells by centrifugation of 1100 g for 20 minutes at room temperature. Supernatant was then centrifuged at 10000 g at 4°C for 7 minutes and pellet with cell debris was then discarded. Finally, plasma samples from each patient were stored at -80°C until use. Moreover, pooled blood samples were used in order to test several different ELISA conditions.

3.2.3 Reagents

The following primary and secondary antibodies were used for exosome characterization in ELISA. Mouse monoclonal antibodies anti-human CD9, CD81 and CD24, Caveolin-1 and Fibronectin were purchased from BD Pharmingen (Milano, Italy). Mouse monoclonal anti-human TSPAN8 was purchased from Sigma-Aldrich (Milano, Italy). Mouse monoclonal antibodies anti-human CD133, PD-L1, CXCR4, EpCAM, Integrin α6, Integrin β4, CD44s and CD44v6 (R&D System, Minneapolis, USA) were reconstituted with sterile PBS to a stock solution. Mouse monoclonal antibodies anti-human CD151 and Alix were from Santa Cruz Biotechnology (Milano, Italy). Goat Anti-Mouse Biotin conjugated was used as secondary antibody (Thermo Fisher, Monza, Italy). Streptavidin Poly-HRP (Thermo Scientific) is used to amplify the signal.

3.2.4 ELISA assay

Transparent Nunc MaxiSorp™ flat bottom 96 well plates (ThermoFisher), with high protein-binding capacity (600-650 ng IgG/cm^2), were used for the ELISA assay according to the following protocol:

1. *Blocking procedure.* 1 hour and 30 minutes at room temperature (RT) under shaking.

   As blocking agents were tested: i) 1% of Bovine Serum Albumine (BSA) protease and fatty acid free (Sigma Aldrich) in PBS, ii) 1% casein (Sigma Aldrich) in PBS, iii) Tween-20 (PanReac Applichem) 0,1% in PBS, iv) 0,2% polyvinylpyrrolidone (PVP) (Sigma Aldrich) in PBS, v) ethanolamine 1M in PBS (Sigma Aldrich).

2. *Washing of the plate*. Three times by using Thermo Scientific™ Wellwash™ Versa Microplate Washer.

   Four different washing buffers were tested: i) PBS with 0,05% of Tween-20, ii) PBS with 0,1% of Tween-20, iii) PBS with a double amount of NaCl (274mM), iv) PBS with a double amount of NaCl (274mM) plus 0.1% Tween-20 (PBST-NaCl).
3. *Sample incubation*. A 100 µl plasma sample from each patient was added to the wells of the plate and incubated overnight at 4°C.
4. *Washing*.
5. *Primary antibody incubation*. 1 µg/ml of primary antibodies was incubated for 3 hours at RT.
6. *Secondary antibody incubation*. 50 ng/ml of secondary antibody biotin conjugate was incubated for 45 minutes at RT under shaking.
7. *Washing*.
8. *Streptavidin Poly-HRP incubation*. 50 ng/ml, 45 minutes at RT under shaking.

The antibodies and HRP were tested in five different dilution buffers: i) PBS, ii) PBS with 0,1% Tween-20, iii) PBS with 0,05% Tween-20, iv) PBS with 274mM NaCl and 0,05% Tween-20, v) PBS with 274mM NaCl, 0.5% BSA and 0,05% Tween.

9. *Washing.*
10. *Substrate addition.* The substrate solution 1-Step™ Ultra TMB-ELISA (Thermo Fisher) was added for 20 minutes at RT under shaking to detect horseradish peroxidase (HRP) activity, yielding a blue colour.
11. *Reactions stop.* A 2M sulfuric acid stop solution was added to each well, changing the blue colour of TMB into yellow.
12. *Measurement.* In order to measure the absorbance (Abs) at 450 nm of each well, Multiskan™ FC Microplate Photometer (Thermo Scientific) was used.

3.2.5 Data elaboration

Absorbance from each well was multiplied by 1000 in order to process data more easily. Absorbance values of the samples (signal) were normalized dividing them by the blank value of the same plate (noise) to obtain the signal/noise ratio.

3.3 Results

3.3.1 Evaluation of the best washing and blocking buffers

The term “blank” refers to those wells where, instead of plasma sample, PBS was added with the aim to quantify only the nonspecific signal due to the binding of the antibodies to the plate surface. The term “signal” refers to the absorbance measured in wells with the plasma samples. One of the goals of the protocol optimization phase is to reduce the absorbance values of the blank wells (noise or background) as much as possible, in order to have the highest signal/noise ratio. Washing and blocking procedures are crucial in ELISA assays to reach this goal.

By using the appropriate washing buffer, it is possible to remove all the unbound molecules in the wells without to dissociate those antibodies specifically bound to the proteins. The washing is performed three times between an incubation and the next. The most common washing buffer is usually PBS with variable percentages of Tween-20. I tested PBS with 0,05% or 0,1% Tween-20 and I found that 0,1% concentration was the most effective in reducing noise. Moreover, the addition of NaCl further helped the reduction of unspecific bounds (data not shown). The last washing was performed without Tween-20 because it has the tendency to inhibit the reaction of HRP with the substrate TMB.

The blocking procedure is useful to saturate the unoccupied spaces of the wells that could interact non-specifically with the proteins. There are various agents that could be used as blockers, usually classified into two major categories: proteins and detergents. Among protein-based agents, BSA and casein were tested and, as non-ionic detergent, 0,1% Tween-20 in PBS was chosen. I have also tested Polyvinylpyrrolidone (PVP), an idrosoluble polymer and the organic chemical compound Ethanolamine. The results of the representative experiment are reported in Table 2, which shows that the most effective blocking buffer is 1% BSA in PBS. Indeed, the absorbance of the blank after BSA treatment was lower (Abs=54) than other blanks (Tween Abs=709; casein Abs=684; PVP Abs=147; ethanolamine Abs=1003). On the contrary, the signals, compared to the blanks, resulted similar or in some cases lower than blanks with all the blocking agents (Tween Abs=739; casein Abs=709; PVP Abs=99; ethanolamine Abs=849) with the exception of BSA (Abs=769).

Blocking	Sample	Absx1000	S/N
PBS+0,1% Tween	Plasma	739	1,04
	Blanck	709	
Casein 1%	Plasma	709	1,04
	Blanck	684	
BSA 1%	**Plasma**	**769**	**14,24**
	Blanck	**54**	
PVP 0,2%	Plasma	99	0,67
	Blanck	147	
Ethanolamine 1M	Plasma	849	0,85
	Blanck	1003	

Table 2 Comparison of different blocking solutions. Human anti-CD9 has been used as primary antibody. Absx1000: Absorbance multiplied by 1000. S/N: ratio of signal (plasma) to blank.

3.3.2 Evaluation of the appropriate antibody dilution buffer

In order to increase sensitivity and decrease nonspecific signals, I needed to test different dilution buffers for the antibodies. First, I compared three different buffers where the primary antibody CD9 was diluted at 1µg/ml: i) PBS, ii) PBS+0,05% Tween and iii) PBS+0,1% Tween. I obtained the highest signal/noise ratio with PBS+0,05% Tween (Plasma Abs=820; Blank Abs=55; S/N=14,91) (Tab. 3). Then, I checked whether there is an improvement by doubling the concentration of NaCl in PBS (referred as 2NaCl-PBS), both with and without 0,5% BSA. According to the results showed in Table 3, I decided to choose the following composition: 2NaCl-PBS + 0,05% Tween + 0,5% BSA (Plasma Abs=890;Blanck Abs=55; S/N=16,18).

Dilution buffer	sample	Absx1000	S/N
PBS	Plasma	760	7,52
	Blank	101	
PBS+0,1% Tween	Plasma	773	12,88
	Blank	60	
PBS+0,05% Tween	Plasma	820	14,91
	Blank	55	
PBS+0,05% Tween	Plasma	815	15,38
	Blank	53	
2NaCl-PBS+0,05% Tween	Plasma	842	13,80
	Blank	61	
2NaCl-PBS +0,05% Tween+0,5% BSA	**Plasma**	**890**	**16,18**
	Blank	**55**	

Table 3 Comparison of different dilution buffers for antibodies. Human anti-CD9 has been used as primary antibody. Absx1000: Absorbance multiplied by 1000. S/N: ratio of signal (plasma) to blank

3.3.3 Characterization of exosome tumour markers from plasma of PDAC patients

After the optimization phase, the customized ELISA protocol was used in order to quantify 16 different exosomal protein markers in plasma samples from 16 PDAC patients. From some patients, only plasma samples before the start of chemotherapy treatment (T_0) and three months after (T_3) were collected, as reported in Table 4. Principal tumour exosome markers were evaluated and their absorbance values were multiplied by 1000 and successively normalized dividing each sample values with the blank value. Patients *P1, P4* and *P5* at the time of the admission in the study had a metastatic disease, whereas *P2* had locally advanced tumour, probably with micro-metastasis as suggested by the CA19-9 serum level. Three months after chemotherapy, these patients showed increased levels of exosomal EpCAM, Integrin β4, CXCR4 and CD24, with the exception of *P5,* who showed lower values at T_3 than T_1 (Tab. 4). However, all patients in this group had a dismal prognosis. For this reason, I assume that the low exosome marker levels in *P5* were due to an error in performing this specific test.

		CD9	CD81	EpCAM	Integrin α6	Integrin β4	CD44v6	CD44s	CXCR4	Tspan8	CD24	CD151	Caveolin
P1	T_0	14,5	3,4	3,2	9,6	2,4	2,1	3,6	5,2	1,7	2,3		
	T_3	12	2,4	17,1	3,7	5,3	2	3,9	17,2	1,4	2,6		
P2	T_0	5,5	4,7	6,3	5,7	5,3	4,5	4,9	5,5	4,2	4,6		
	T_3	10,5	4,9	20,7	6,1	11,2	5,1	6,2	17,6	2,9	4,7		
P4	T_0	8,3	3,5	2,9	3,3	2,3	2	3,4	5,3	1,9	2,1		
	T_3	13,9	3,1	13,5	4	4,4	2	2,7	14,8	1,3	2,7		
P5	T_0	18,6	3	21,4	4,4	6,5	2,5	3,3	17,5	1,9	4,3	1,8	2,6
	T_3	26,8	5,3	1,7	1,6	1	5,4	2,1	8	3,4	3	1,7	0,7

Table 4 Principal exosome markers evaluated in plasma samples of PDAC patients (P1, P2, P4, P5). Blood samples taken at the start of chemotherapy (T_0) and three months after the treatment (T_3). Numbers refer to Abs values x 1000 normalized for the blank values.

Successively, in order to better analyse the effects of treatments and the disease progression, blood samples were also taken at the one month (T_1), two (T_2) and three (T_3) months timepoints after chemotherapy. T_3 is when the patients had to undergo to radiological evaluations. Blood samples were also taken at six (T_4) and eight (T_5) months, when possible (Tab. 5a, 5b, 5c).

Patient *P3* had locally advanced disease (T_0) and, as well as *P2*, its plasma levels of EpCAM, Integrin β4, CXCR4 and CD24 increased at T_3 timepoint. However, these markers showed a decrease at T_4 that was unexpected since *P3* also progressed and died. Patient *P6* had been diagnosed with metastatic pancreatic ductal adenocarcinoma at the admission in the study (T_0). Our test showed that only Integrin α6 and CXCR4 increased, whereas other markers such as EpCAM, Integrin β4, CD151 decreased their levels. At the follow-up, the tumour showed signs of progression but, however, it seems that palliative chemotherapy had shown efficacy since *P6* is still alive. Exosome markers remained unvaried for the patient *P7*, with the exception of CXCR4, which showed a slight increase. *P7* is the only patient with resectable tumour and no signs of disease relapse. *P8* patient, with metastatic disease, showed increased levels of different exosomal markers: EpCAM, CD44s, CD24 and CD151. At the follow-up (T_3), CD44v6 had been decreased, probably due to a beneficial effect of chemotherapy, but at T_5 its level recurred high as at the T_0. *P8* had a progression even if its survival was longer than the other patients (Tab. 5a).

Patients from *P9* to *P16* have been diagnosed with metastatic disease. Levels of CD44v6 and Tspan8 increased at the follow-up in *P10, P12, P13, P14* and a growth of EpCAM and CD24 in *P10, P12* and *P13* was observed (Tab 5b, 5c). Patient *P16* have showed reduced levels of EpCAM, CXCR4 and CD24 while Integrin β4, CD44v6 and Tspan8 increased (Tab 5c). In this group, *P10* and *P16* displayed a progression at three months and *P12* at the follow-up, successively *P10* and *P12* died.

Interestingly, I observed that immediately after chemotherapy (T_1) some of the exosome markers showed a decrease of levels in plasma patients, followed by a growth after two or three months. In particular, exosome markers that followed this trend were: CD24 (*P6, P7, P13, P14, P16*), CD151 (*P7, P10, P12, P14, P16*), Integrin β4 (*P8, P12, P14, P16*), CD44v6 (*P6, P10, P13, P16*), Caveolin-1 (*P7, P10, P14, P16*), PD-L1 (*P7, P10, P14, P16*), Integrin α6 (*P6, P14, P16*) and CD133 (*P13, P14, P16*). Their trend

could be connected with the worsening of the health conditions and to the poor survival, indeed *P6*, *P8, P10, P16* progressed under chemotherapy treatment and *P10* died.

		CD9	CD81	Epcam	Integrin α6	Integrin β4	CD44v6	CD44s	CXCR4	Tspan8	CD24	CD151	Caveolin	PD-L1	ALIX	CD133	Fibronectin
P3	T_0	6,2	2,8	2,5	3,9	1,8	1,6	2,5	5,1	1,4	1,8	1,5					
	T_3	7,3	3,6	16,3	2,5	4,8	1,7	3,4	15,3	1,4	3,2	1,2					
	T_4	10,4	4,7	2,7	1,7	0,3	1,4	2,6	5,2	1,3	1,2	1,3	1,3				
P6	T_0	26,5	5,1	4,7	1,2	2,5	2,8	3,6	2,6	5,9	1,8	2,6	1,6	0,8			
	T_2	24,8	6,3	2,6	1,0	1,8	1,2	4,0	3,2	7,7	1,6	2,2	1,8	1,1			
	T_3	32,1	4,7	2,1	2,4	1,8	1,1	4,1	3,5	6,8	1,8	1,8	1,1	0,7			
	T_4	4,1	4,6	1,3	7,6	1,8	1,9	3,5	8,8	0,9	1,8	1,8	1,5	2,5	1,4	3,2	5,3
P7	T_0	24,4	13,4	6,7	2,4	1,7	2,0	3,6	4,0	6,1	4,6	4,1	2,7	2,2			
	T_1	22,6	12,2	7,0	2,9	3,1	2,1	2,7	4,7	6,3	2,6	3,6	1,8	1,4			
	T_2	23,4	15,4	5,4	2,1	2,4	2,3	2,5	5,1	7,2	3,0	4,1	6,7	3,5			
	T_3	16,3	13,2	5,0	1,5	1,9	1,8	3,2	6,4	6,0	3,3	3,0	2,8	2,1			
P8	T_0	35,5	14,7	1,0	2,1	3,0	3,6	4,0	8,7	1,7	2,8	1,3	1,1				
	T_1	38,5	8,2	1,2	2,1	1,1	5,6	3,1	8,6	3,9	3,0	1,7	0,9				
	T_2	7,3	6,2	1,3	9,1	1,8	1,6	4,7	9,6	0,8	1,3	1,4	1,8				
	T_3	12,6	5,7	1,3	5,3	1,9	1,9	5,2	8,4	0,9	1,8	1,6	1,9				
	T_4	17,9	13,7	3,9	2,6	1,8	2,6	11,4	2,9	2,1	4,6	2,3	1,9	2,8	3,3	4,5	7,2
	T_5	20,8	6,5	2,4	1,5	2,6	3,4	4,5	1,5	1,6	3,3	1,9	1,6	2,7	2,3	4,0	7,5

Table 5a

		CD9	CD81	Epcam	Integrin α6	Integrin β4	CD44v6	CD44s	CXCR4	Tspan8	CD24	CD151	Caveolin	PD-L1	ALIX	CD133	Fibronectin
P9	T_0	13,9	8,9	8,3	2,8	3	2,7	7,6	3,8	3	8,3	4,1	2,9	5,7	3,3	5,4	7,8
	T_1	9,1	6,3	6,3	2,4	2,3	2,4	5,6	2,6	2,2	4,2	3	3,4	4,9	2,6	3,4	4,7
P10	T_0	11,2	9,8	2,1	7	3,4	3,1	8	9,1	1,7	2,9	3,1	3,7	2,8	2,4	3,8	14,8
	T_1	12,9	10,9	1,6	7,1	3	3,1	9,1	8,6	1,5	2,7	2,8	2,8	2,4	2,6	3,9	18,5
	T_2	10,1	11,3	1,8	8,4	3,5	3,1	11,3	9,3	1,6	2,9	3	4,6	2,5	2,6	3,3	13
	T_3	10,8	11,4	4	3,6	3	4	11,9	3,3	3	4,1	3,8	3,2	4	3,5	4,1	9,6
	T_4	21,6	9,6	4,7	2,1	3,3	3,8	6,3	2,2	3	4,5	3,5	2,7	4,6	4,4	5,4	9,9
P11	T_0	17,9	5,8	2,8	2,3	1,8	2,2	4	2,5	2,2	3,5	2,2	2,1	2,9	2,6	3	4,7
	T_1	4,7	5,5	2,7	1,5	1,5	1,6	2,6	1,8	1,6	2,2	1,7	1,5	2,2	1,6	2,3	4,3
P12	T_0	10,3	4,4	1,2	8,7	1,9	1,5	3,3	8,1	0,9	1,5	1,5	3,9	2,2	1,2	3,1	6,3
	T_1	11,1	5,3	1,3	7,5	1,9	2,8	3,7	9,8	1	1,7	1,4	2,1	2,5	1,3	2,9	7,8
	T_4	4,9	2,6	2	0,9	4,3	2,6	2	1,1	2,1	2	1,6	1,4	2,3	1,4	2,8	2,5

Table 5b

		CD9	CD81	Epcam	Integrin α6	Integrin β4	CD44v6	CD44s	CXCR4	Tspan8	CD24	CD151	Caveolin	PD-L1	ALIX	CD133	Fibronectin
P13	T_0	15,9	6,6	1,4	1,5	1,7	3,5	2,6	1,5	1,8	6,3	2,1	2	2,2	1,7	2,8	10,7
	T_1	37,5	6,7	1,6	2	1,7	2,7	3	1,5	2,1	5	2,1	2	2,3	2,3	2,5	12,4
	T_3	30	8,9	2	1,1	1,7	3,3	4,6	1,8	2,2	7,1	1,8	1,7	3,1	2,1	4,9	6,6
P14	T_0	19,7	12,4	2	1,5	1	1,3	1,1	2,2	1	5,3	5,8	1,4	1,6	1,3	2,7	17,4
	T_1	8	3,9	2,2	1,1	1	1,4	3,1	2,2	0,9	2,3	1,1	1,2	1,5	1,5	1,6	16,1
	T_3	15,1	4,6	1,4	1,5	1,4	3,3	1,9	1,4	1,5	2,8	1,7	1,6	2,5	1,6	2,7	4,3
P15	T_0	7,3	5,8	2,2	1,3	1,1	1,3	7,8	2,6	1,3	3,1	1,2	1,7	2	1,3	2	13,6
	T_1	6,6	7,7	2,4	1,2	1	1,6	4,8	2,4	1	2,5	1,2	1,3	1,7	1,7	1,9	16,2
P16	T_0	26,3	8,4	2,6	2,6	1,5	2	9,2	2,9	1,2	10,2	2,6	3,6	3,1	3,7	6,9	23,9
	T_1	45,3	6	2,5	1,8	1,1	1,8	6,4	2,6	1,3	5,8	1,8	2,3	2,2	2,2	3,2	14,2
	T_3	21,4	5,5	1,8	2,3	2	3,1	4	1,9	2,6	7,1	2,4	4	2,5	2,6	3,7	8,5

Table 5c

Principal exosome markers evaluated in plasma samples of PDAC patients (*P3, P6-P16*). Blood samples taken before chemotherapy (T_0), at one month (T_1), two months (T_2), three months (T_3), six months (T_4) and eight months (T_5) after chemotherapy. Numbers refer to Abs values x 1000 normalized for the blank values.

3.4. Discussion

3.4.1 Elisa assay development and optimization

Enzyme-linked immunosorbent assay (ELISA) is a quantitative technique, highly specific and sensitive, which allows the measuring of molecules of interest even using complex matrices such as human plasma or serum. However, it is a time-consuming procedure because it consists of various incubation steps, one overnight, alternated with several washings, and it requires an extremely high precision from the operator in order to have all the wells comparable and reliable. Moreover, due to the high capacity of the plate to bind proteins, it is easy to detect false-positive results. For these reasons, before starting with the actual measurements of samples from the patients enrolled in the study, I performed different experiments in order to detect only exosomal proteins and minimizing unspecific signals.

Washing procedures are crucial in removing all the unbound proteins. It is important that all the wells are filled with the same volume, soaked for the same time and eventually quickly and simultaneously emptied. The microplate washer, used in this work, helped to perform this procedure in a standardized manner, which guarantees that the different signals among wells are not caused by different washing intensity. Commonly, a solution of PBS and Tween-20 is used for the washing method. I found that an increased concentration of NaCl into the buffers provides a better washing. The comparison among different buffer compositions led me to choose a composition of PBS with 274mN NaCl (2NaCl-PBS) with the addition of 0,1% Tween.

The absence of standardized blocking procedures suitable for all the ELISA applications is well known. The two major classes of blocking agents are detergents and proteins. Regarding the first class, non-ionic detergents such as Tween-20 or Triton-X, are the most used but they are considered weak blockers that do not offer a stable barrier. This consideration is congruent with the results showed in Table 2, where blocking with Tween-20 gave comparable absorbance values between sample and PBS incubation. On the contrary, proteins are permanent blockers and the most widely used for ELISA assays as reported in literature [69, 71, 75-77]. Here I compared two different types, bovine serum albumin and casein. Although both determined the same signal intensity with plasma, somehow primary or secondary antibodies bound unspecifically with casein but not with BSA, as showed in Table 2. An alternative

compound, not belonging to the two already mentioned classes, is Polyvinylpyrrolidone (PVP), a water-soluble polymer that has already shown good blocking properties in some studies for its ability to cover hydrophobic surface and to detect small proteins [78-80]. Here, PVP prevented plasma proteins to bind to the well (Abs= 99) while the corresponding blank well resulted in a slightly increased signal (Abs= 147); these outcomes highlighted that PVP is not an ideal blocker for the experimental setup used in this study. Ethanolamine, even if used in immunoaffinity assays, did not appear suitable for the blocking process (plasma Abs= 849; blanck Abs=1003). According to the results obtained, I used BSA for the analysis with PDAC plasma samples.

Finally, I needed to test different compositions of the dilution buffer for the antibodies. Table 3 shows that higher concentration of Tween-20 may inhibit the specific binding antigen/antibody. As a compromise, I chose a smaller percentage (0,05%) of Tween-20 because using only PBS the sensitivity was reduced. Then, I tested the effect of the increased concentration of NaCl into the buffer (2NaCl-PBS) with or without a small quantity of BSA. I found that the buffer composed of 2NaCl-PBS + 0,05% Tween-20 + 0,5% BSA guaranteed the specific signal of the antibodies and suppressed the background. The positive cooperation of NaCl and BSA in dilution buffers was also previously described [81].

These experiments demonstrated the importance of verifying the suitability of each component in an ELISA assay, especially when biological matrix are analysed, since by using different agents it is possible to obtain different outcomes that could completely alter the final interpretation.

3.4.2 Exploring correlations between exosomal markers and clinical variables

Pancreatic ductal adenocarcinoma is one of the most aggressive gastrointestinal tumours, with a five-year survival rate of 6%. It is often diagnosed at an advanced stage, when only chemotherapy treatment is possible, whereas only 10-20% of patients have resectable disease. Exosomes have been considered interesting tumour markers that could be quantified in a non-invasive way in human body fluids. In this work, I investigated the relation between the levels of exosome in plasma samples, measured by ELISA assay using principal exosome proteins, and the therapeutic

outcomes. Fifteen patients with metastatic or locally advanced pancreatic ductal adenocarcinoma that could be treated with palliative chemotherapy and one patient that had received radical surgery of the tumour were enlisted in this study. Plasma samples from each patient were split with other two research groups, involved in the same project, in order to carry out further analysis regarding circulating tumour cells (CTC) and exosome miRNA profiling. For this reason, the received volume of plasma was not enough to perform replicates of each protein marker. Moreover, PDAC patients were, at the time of admission in the study, in different health conditions (Tab. 1) that make it difficult to compare exosome plasma levels at T_0. Furthermore, we expected that the number of enrolled patients was substantial in order to effectively detect correlations between exosomal markers and clinical variables.

In our results, it emerged that at T_1 some of the exosomal markers underwent a decrease, leading me to suppose a positive chemotherapy effect. However, after only two or three months, CD24, CD151, CD44v6, Caveolin-1, Integrin β4 and PD-L1 started to increase their levels in some patients in parallel with their health state worsening. These proteins could be considered candidate biomarkers in PDAC. In a recent study, it has been demonstrated that anti-myeloma drugs stimulated secretion of cancer exosomes with altered composition, leading to tumour cells survival and chemoresistance [82]. It could be possible that chemotherapeutic agents used in PDAC treatment enhanced secretion of exosomes by tumour cells, implicating an exacerbation of the disease status in examined patients.

Among exosome proteins evaluated in this work, CD24, CXCR4, EpCAM, CD44v6 and Tspan8 may be biomarker candidates for pancreatic cancer since they exhibited a steady growth starting from T_0 in our patients.

CD24 is a surface marker of cancer stem cells and it has been found expressed in several pancreatic cancer cell lines [83]. It was recognized as a cancer marker, associated with poor prognosis, in ovarian carcinomas and it could have been released into the extracellular environment via exosomes because it was found in the cytoplasm inside MVBs [83, 84]

In some patients (*P2, P4, P6, P7, P13*), CXCR4 showed an increase of its plasma level at the follow-up. CXCR4 could be a potential marker of tumour relapse or progression. It should be noted that the CXCR4 increase occurred also in *P6* and *P7* that are,

respectively, the patients with a prolonged survival and resectable tumour, suggesting that their disease could have progressed. CXCR4 is a G protein-coupled chemokine receptor that is upregulated in migrating cancer stem cells and its involvement has been suggested in angiogenesis, tumour growth and therapy resistance. It has been demonstrated, by immunohistochemistry or microarray analysis, that its expression is increased in 85% of pancreatic cancers revealing its role as prognostic biomarker [74, 85, 86]. In another work, immunohistological staining of pancreatic tissues from PDAC patients have revealed that CXCR4 expression significantly correlated with lymph node metastasis [87]. A comprehensive study that performed a meta-analysis by pooling CXCR4 expression data obtained from nine different works confirmed the correlation of CXCR4 expression and pancreatic cancer poor prognosis [88].

EpCAM could be also considered a biomarker since my assays have reported a steady increase of its levels in most cases, while in *P6* and *P7* resulted to be reduced. EpCAM, a transmembrane protein, is a known marker of cancer stem cells in pancreatic, liver, colorectal and breast cancers [74]. EpCAM, together with CD44v6, has been shown to have an increased expression in Panc1 cancer stem-like cells [89]. Recently, a proteomic analysis of exosomal membrane has revealed that EpCAM is one of the PDAC biomarker candidates, together with CD151, in liquid biopsies from patients [90]. Patients *P2, P5, P11, P13, P15*, showed an increase of CD44v6 levels at T_3 timepoint that could confirm the previous findings that associated CD44v6 with more aggressive tumours and metastasis [73].

Tspan8 is a tetraspanin found in tumor-derived exosomes that is involved in epithelial cells proliferation and angiogenesis induction [91]. In this study, Tspan8 values resulted increased in some patients (*P5, P10, P12, P13, P14, P16*) that have not responded to the therapy.

In conclusion, this method has provided a first approach for analysing, in plasma samples, changes of exosome levels comparing them with the disease status of patients in order to find candidate biomarkers of PDAC. However, specific correlations have not been highlighted and sometimes problems emerged, for example some values at T_3, or at successive timepoints, were low even though patient conditions were not improved. This could be caused by different plate conditions that may alter ELISA results. Moreover, the upstream procedures are crucial to make tests more

comparable. It is very important to standardize the sampling phase since many factors, such as fasting or postprandial status of the patients, could influence the extracellular production by cells [22]. In addition, plasma extraction should be done in the shortest possible time after blood sampling because blood cells continue to release exosomes during blood storage, thus altering exosome populations [22].

However, in order to validate the results about exosomes in plasma samples, additional replicates would have been necessary.

4 Identification of gene and miRNA biomarkers for pancreatic ductal adenocarcinoma by weighted gene co-expression network analysis

4.1 Introduction

Microarray technology is a method that has been widely used in the last decade which allows researchers to investigate the simultaneously expression levels of more than 20000 genes in a sample. Many statistical methods proposed for microarray data analysis have permitted to identify, among groups of samples (for examples healthy and disease samples), individual differentially expressed genes that may provide biologically and pathologically relevant information. When differentially expressed genes are identified it is possible to perform the functional enrichment analysis in order to highlight pathways and biological processes where the identify genes are involved. This analysis is usually carried out by web tools such as GOrilla, GSEA, DAVID or Ingenuity Pathway Analysis, that are based on GeneOntology terms and KEGG and Reactome pathway databases. However, the main problem of the interpretation of microarray-based expression data is that only individual genes and not the correlation among them are considered, causing often a wrong explanation of biological phenomena.

The network analysis, on the contrary, interprets gene expression data with a global approach introducing the connections among genes [92]. A gene co-expression network is an undirected graph, constituted by nodes (genes) that, if they are highly co-expressed, are connected with edge (link) without orientation. This graph can provide several biological information: co-expressed genes can be under the control of the same transcription factors, involved in the same functions or can be members of the same protein complexes or pathways[93].

The weighted gene co-expression networks analysis (WGCNA) is one of the primary methods, together with Bayesian networks, used to deduce gene networks from microarray-based data. WGCNA is based on the concept of a scale-free network with the presence of a few highly connected nodes (hubs) with many others poorly connected nodes. Such network is robust with respect to the random deletion of nodes, but is sensitive to the targeted attack on hub nodes. WGCNA assumes that all

genes are connected with a different weight which is quantified from the correlations of their co-expression. Highly co-expressed genes connected in a network, i.e. hubs with an extensive number of links, can be grouped into modules (highly connected regions of the network) which may correspond to clusters of functionally related genes. Detecting modules is one of the objectives of WGCNA [92, 94]. This approach can be applied to two groups of samples, for example healthy and diseased samples, in order to acquire a network for each group and identify the modules that differ between the groups. Within each unconserved module, the identification of the hub molecules could be useful to find new diagnostic/prognostic biomarkers or novel drugs that could target them. WGCNA has been widely employed in oncology in order to find cancer-risk modules in various tumours [95-97].

During my PhD, I applied for the first time the weighted gene co-expression analysis to PDAC-derived data. The results have been published in the Cellular Oncology journal [26, 27]. In particular, I have analysed microarray-based gene and miRNA expression profiles from tissues and serum samples of PDAC patients and healthy individuals. I have applied WGCNA to identify key genes and miRNAs potentially involved in the pathogenesis of PDAC and I have also validated them as prognostic biomarkers.

4.2 Materials and Methods

4.2.1 Gene and miRNA expression data and pre-processing

Datasets used in this work were downloaded from NCBI Gene Expression Omnibus (GEO). In particular, five microarray-based gene expression datasets composed of expression data from 105 normal pancreatic and 129 PDAC tissue samples: GSE15471 [23], GSE32676 [24], GSE28735 [25], GSE41368 [98] and GSE71989 (unpublished). Quantile-normalized miRNA expression data were acquired from GSE59856 dataset which contains serum samples from 150 healthy donors and 100 PDAC patients [99]. This dataset was produced using the microarray platform 3D–Gene Human miRNA V20_1.0.0 and was based on miRNA sequences listed in a recent release (v20) of the miRBase database (www.mirbase.org) for probe design, which allows the expression assessment of 2555 miRNAs. Data analyses were performed using the R 3.1.2 statistical environment (www.r-project.org) and Bioconductor (version 2.14) (www.bioconductor.org). Raw data from each microarray dataset were pre-processed with the R package *affy* using the Robust Multichip Average (RMA) function for background correction and normalization with the quantiles method [100]. Since the microarray datasets were obtained from two different platforms, they were made compatible with the purpose of merge them. We first mapped the array probes to the respective Entrez Gene ID, a cross-platform common identifier, using the array annotation data hgu133plus2.db or hugene10sttranscriptcluster.db, depending on the platform used. Then, we summarized the expression values of given genes, measured by multiple probes, using the function *collapseRows* implemented in the R package WGCNA [101]. We selected the parameter *"MaxMean"* which chooses the probe with the highest mean value among samples, since this generally produces the most robust results [102]. We created an overlapping gene set, to limit further analyses to genes present in all datasets, by selecting the rowTs with the Entrez Gene ID present in both platforms using the WGCNA function *intersect*, resulting in a total of 17,536 common genes. Since in the Affymetrix Human Gene 1.0 ST are represented 19,878 and in Human Genome U133 Plus 2.0 Arrays there are 19,851 unique Entrez Gene IDs, the percentages of common genes included in our analyses are considered to be very high (88.2 and 88.3). The cross-platform batch effects were removed with the *ComBat* method, chosen among other methods, because it reaches the highest precision,

accuracy and overall performance. *ComBat* is implemented in the R package *sva* and executes another normalization step using an empirical Bayes approach [103, 104]. After this, all normalized microarray-based data could be merge into two global datasets: Normal and PDAC, that we used for the subsequent WGCNA analyses.

In order to detect outlier samples, the standardized connectivity (Z. K) method was followed. The Z.K score represents the overall strength of connections between a given node and all of the other nodes in a network, samples with a Z. K score < −2 have to be considered as outliers [105].

4.2.2 Dataset comparability analyses

It is necessary, for the following analyses, to assess the comparability between Normal and PDAC datasets from pancreatic tissues and among the two datasets of healthy donors and PDAC serum samples. To this end, the *softConnectivity* function from package *WGCNA* permitted to evaluate the correlation of the expression level of each gene or miRNA and the correlation of the overall connectivity, across the datasets. This serves to assess comparability between normal and PDAC samples. If the two correlations are positive and the *p*-values significant, the two datasets are comparable. Higher correlation values (ranging from 0 to 1) indicate higher comparability between the normal and PDAC datasets. For WGCNA analysis it is required that the topology of the networks is scale-free, and therefore we applied the *pickSoftThreshold* function of the *WGCNA* which provides a *Scale-free Topology Fit Index.* If the index reaches values above 0.8 for low power (< 30) it means that the topology of the network is scale-free [94].

4.2.3 Construction of weighted gene co-expression networks and their modules

Using standard WGCNA procedures [94], we created, both for gene and miRNA expression data, two weighted gene co-expression networks based on Normal and PDAC data, respectively.

In each dataset we first created a matrix of adjacencies through the WGCNA function *adjacency,* then this matrix was transformed into a Topological Overlap Matrix (TOM) using the function *TOMsimilarity*. The topological overlap indicates the gene similarity based on co-expression relationships between two genes [94]. Each TOM was used as input for hierarchical clustering analysis, which has been performed with the function

flashClust. Finally, in the resulting dendrograms I identified network modules present in the Normal dataset (used here as reference dataset) with the function *cutreeHybrid* from the R package *dynamicTreeCut*, using a relatively large minimum module size (minClusterSize = 30), and a medium sensitivity (deepSplit= 2), with other parameters set as default.

4.2.4 Modules preservation analyses

The preservation levels of Normal network modules in the PDAC network were evaluated by the function *modulePreservation* from the WGCNA package. In particular, it performs a permutation test which assesses the preservation of the connectivity and density between each couple of modules, each belonging to the Normal and PDAC networks. This functions provided a preservation Z-score for each module. High Z-scores (> 10) indicate that the modules are well preserved between normal and PDAC networks, whereas values lower than 10 are indicative for a moderate to low preservation [106]. The grey and gold modules are special WGCNA modules that were not considered.

4.2.5 Detection of hub genes and their functional annotation

Intra-modular highly connected genes are defined as hub genes with the highest Module Membership (MM) scores to the respective module [107]. The MM was calculated with the *WGCNA* function *signedKME* that correlates the expression profile of a gene with the Module Eigengene (ME) quantifying how close a gene is to a given module. ME is calculated by the *WGCNA* function *moduleEigengenes*. ME is a virtual gene which represents the gene expression profile of the entire module. We mapped these genes to the associated Gene Ontology (GO) terms and KEGG pathways using the DAVID tool (http://david.abcc.ncifcrf.gov/) [108]. For each non-preserved module I selected the 20 most connected hub genes. Then I performed functional enrichment analyses for the interpretation of the biological mechanism related to a given gene list. Enrichr tool (http://amp.pharm.mssm.edu/Enrichr/) [109] was used to perform enrichment analyses of our hub gene lists. The enrichment analyses were executed on predicted transcription factor binding sites using the “TRANSFAC_and_JASPAR_PWMs” section, on predicted miRNA binding sites using the “TargetScan_microRNA” section, and on chromosomal regions where these genes are located using the

"Chromosome_Location" tool section. Only statistically significant results are reported ($p<0.02$).

4.2.6 Detection of hub miRNAs and their functional annotation

The WGCNA functions *moduleEigengenes* and *signedKME* were used to identify hub miRNAs. Then, we selected the 20 most connected hub miRNAs for each non-preserved module. Next, we carried out functional enrichment analyses of known miRNA targets in order to facilitate the interpretation of the biological functions related to these miRNAs. The most interesting miRNAs were used as input for the miRNet web tool [110] to identify the biological pathways, processes, molecular functions and cellular components statistically enriched for the corresponding miRNA target genes. In particular, this tool identifies the enriched KEGG and REACTOME pathways and Gene Ontology (GO) terms based on miRNA targets. Since this tool utilized experimentally validated miRNA targets, it guarantees a higher reliability than tools based on predicted miRNA targets.

4.2.7 Survival analyses

SurvExpress tool was used for the survival analyses [111] which allows comparisons and validations of candidate genes as cancer prognostic biomarkers using patient survival data present in other microarray datasets. This tool splits samples into high-risk and low-risk groups through the median of the prognostic index obtained via a Cox regression model. Then, risk hazard ratios (HR), relative confidence intervals (CI) and *p*-values are generated. Survival analyses were performed on an independent GEO dataset (GSE21501), containing gene expression and survival data derived from 132 PDAC patients.

Instead, for the validation of the identified hub miRNAs as prognostic PDAC biomarkers, we used the SurvMicro web tool [112] in order to perform survival analyses similarly to the SurvExpress tool. It was carried out on an independent PDAC dataset present in The Cancer Genome Atlas (TCGA) (http://cancergenome.nih.gov/) containing miRNA expression and survival data derived from 54 PDAC patients.

4.3 Results

4.3.1 Pre-processing of the Normal and PDAC dataset

Five microarray datasets composed of raw gene expression data from normal and pancreatic cancer tissue samples were pre-processed and merged into two global datasets: Normal and PDAC. This step was necessary since WGCNA is sensitive to batch effects (systematic and technical differences among different datasets) and to the presence of outlier samples [94]. The Normal dataset included 104 samples and the PDAC dataset 129 tumour samples. Then, I evaluated their comparability, since high comparability provides better chances of finding similarities and differences between datasets during subsequent analyses. I showed that our datasets are comparable, with a correlation of gene expression of 0.97 ($p<1e-200$) and gene connectivity of 0.43 ($p<1e-200$). The latter parameter indicates the weighted co-expression level correlation that means how strongly a gene is connected to all other genes in the network.

Successively, I checked if the networks to be constructed had a scale-free topology, a requisite of metabolic and signalling networks in which some nodes (here genes) are more connected than others, so that some nodes are central (hub nodes) and others are peripheral. For this aim, we used the R function *pickSoftThreshold*. It was found that the scale-free topology fit index correctly reached values above 0.8 for a low power of 10 in the Normal dataset, here used as a control dataset (Fig. 1 A). This result is an indirect sign that the batch-effects were efficiently removed.

The GSE59856 dataset [99] includes miRNA expression data of serum samples from 150 healthy donors and 100 PDAC patients. This dataset evades from the batch effect because it is formed of the same type of microarray accomplished by the same operators. Regarding the presence of outliers, 6 and 5 samples were removed respectively from normal and PDAC datasets.

Since it is required for WGCNA, the datasets were confirmed to be highly comparable by the *softConnectivity* function. Indeed, the overall miRNA expression correlation was 0.85 ($p<1e-200$) and the overall miRNA connectivity was 0.3 ($p<3.3e-51$).

Moreover, we found that the Normal network showed a scale-free topology with the Scale-free Topology Fit index above 0.9 for low powers of 7 (Fig. 1 B). This result also confirmed the no batch-effects in the original microarray datasets.

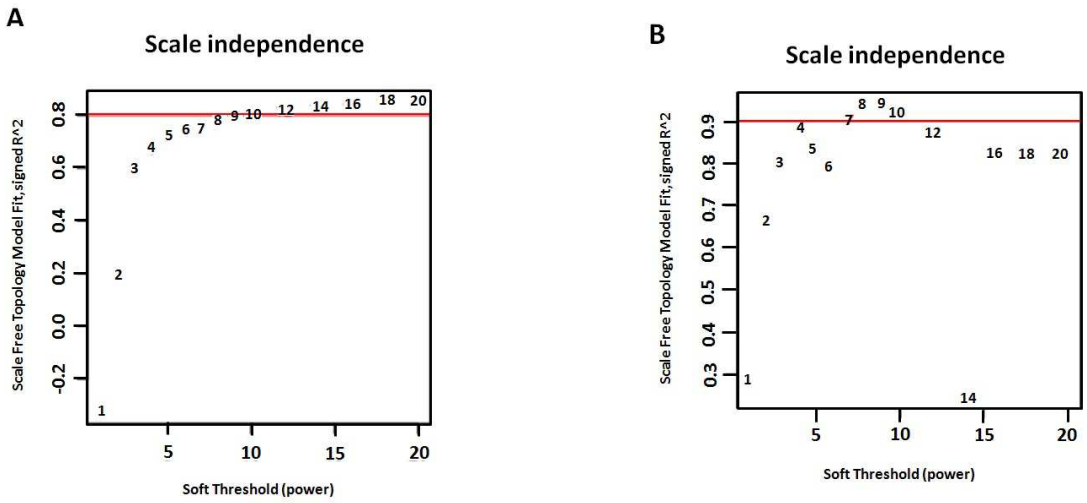

Figure 1 Identification of the optimum soft-threshold power by calculation of scale-free topology fit index. Values of the corresponding soft threshold power are shown. In panel A the optimum power value is 10 since it is the minimal value above the guidance line set at 0.8 in the Normal dataset of gene expression data. In panel B, for the Normal dataset of miRNA expression data, the optimum power value is 7 since it is the minimal values above the guidance line set at 0.9.

4.3.2 Weighted gene and miRNA co-expression networks and their modules

In WGCNA, a module is a group of strongly co-expressed genes that generally have similar biochemical and functional properties or are linked in the same pathway [113-115].

In the Normal gene dataset, we identified, via hierarchical clustering, 26 modules. Then, we evaluated how the characteristics of the identified modules in the reference network (Normal) are reproduced in the PDAC dataset used as test network (preservation level). This way, it is possible to recognize in PDAC networks the altered modules. The *modulePreservation* function from the *WGCNA* package permitted to quantify the module preservation and to identify lowly preserved modules by calculating a Z-scores for each module that is higher than 10 for those highly preserved (Tab. 6). Lowly preserved modules between datasets are the *mod25* (Z-score = 9.6) and *mod26* (Z-score = 8.4) and they may distinguish normal from pathological conditions. Regarding miRNA datasets, 12 modules were identified with different miRNA number in the normal network. Then the preservation level across the two networks was assessed and, as expected, some modules possessed similar characteristics in both

networks but others, which were not preserved, are probably related to the development of PDAC. According to the Z-scores calculated by *modulePreservation*, the *M3* and *M4* modules and *Meta-mod* (which includes: *M12*, *M11*, *M10*, *M7*, *M6*, *M2*) were found to be not preserved (Tab. 7) (Fig.2).

Module	**Z-score**
mod1	44,7
mod2	36
mod3	32,9
mod4	30,1
mod5	28,4
mod6	27,8
mod7	27,5
mod8	26,1
mod9	25,3
mod10	25,2
mod11	23,5
mod12	20,7
mod13	19,4
mod14	18
mod15	17,4
mod16	15,6
mod17	14,9
mod18	13,5
mod19	12,9
mod20	12,6
mod21	12,1
mod22	11,7
mod23	11,6
mod24	10
mod25	9,6
mod26	8,4

Table 6 Modules identified in the Normal network by *WGCNA* functions and relative preservation (Z-score). Modules with Z-score>10 are preserved modules that well maintain their characteristics in the PDAC network. Modules with Z-score<10 are low preserved, so they can distinguish normal and pathological conditions.

Module	Z-score
M1	16,1
M8	15,3
M9	12,4
M5	11,5
M11	6,5
M12	4,7
M3	4,3
M10	3,7
M2	3,5
M4	2,0
M6	1,2
M7	0,5

Table 7 Modules identified in the Normal network and relative preservation. Z-score>10 are the defined modules that well maintain their characteristics in the PDAC network. Modules with Z-score<10 are low preserved.

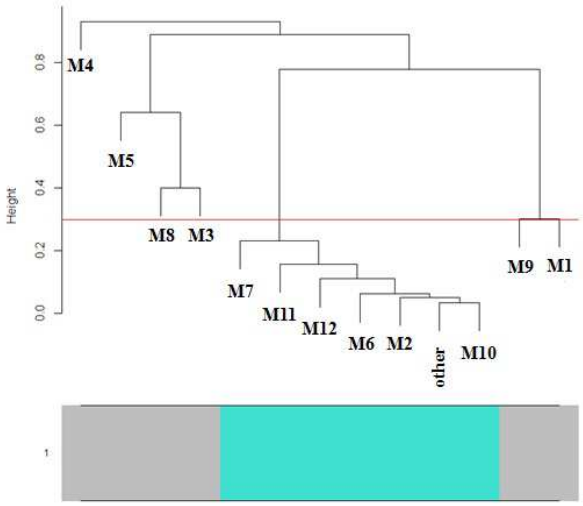

Figure 2 Meta-module identification. The horizontal line represents the threshold (0,3) used for defining the meta-modules. The *M12*, *M11*, *M10*, *M7*, *M6*, *M2* modules represent a meta-module (hereafter referred to as *Meta-mod*) in the PDAC network. *Other* is the module of miRNA not assigned to any module, and should not be considered for the following analyses.

4.3.3 Identification of hub genes and their functional annotations

For each module, the hub genes present in both networks has been identified. Next, the *mod25* and the *mod26* modules, found to be lowly preserved, were further analysed since they can potentially distinguish PDAC from normal samples. In particular, 20 hub genes in each module (listed in Table 8) identified exclusively in the PDAC network might be involved in the pathogenesis. DAVID tool was used for a functional enrichment analysis in order to find out the biological functions associated with these hub genes. Enriched Gene Ontology (GO) terms with *p*-value<0.05 were listed in Table 9. Hub genes related to endoplasmic reticulum were the significantly over-represented genes in the *mod25* module, while some GO terms in the *mod26* module are related to cellular compartment such as cytoplasm, membranes or mitochondria, others are related to biological processes: lipid metabolism, transferase activity, hydrolase activity and transmembrane transport. The Enrichr tool was used to perform a gene enrichment analysis to identify common elements involved in gene expression regulation. The transcription factors most over-represented in both modules and statistically significant were RBPJ and FOXO3A (Tab. 10) and, regarding microRNAs, miR-202 were found to be enriched in the *mod25* module (p = 0.0112). Its predicted targets are the BCL7A and MANEL genes. The chromosomal regions 7q21 and 3q28 were found to be enriched in genes from the *mod26* module: PON2 and SLC25A13 (p = 0.0012) and B3GNT5 (p = 0.0115), respectively. The chromosomal region 20q13 was found to be enriched in genes belonging to the *mod25* module: STAU1 and ZNF334 (p = 0.0064).

Module	Hub genes
mod25	BCL7A, C15ORF52, CAMKMT, CEP170B, ERLIN2, KCNMB3, LARP1, LRRC8E, MANEAL, POLDIP2, SEC23B, STAU1, TBC1D24, TBL2, TMEM51, TTC30A, TXNDC12, VWA8, ZDHHC4, ZNF334
mod26	B3GNT5, BPNT1, C2ORF47, CASK, CEACAM1, CERS6, CYCS, DNAJC15, ELOVL6, FLVCR1, MCU, MFSD6, MRPS36, NAPEPLD, PON2, SLC25A13, TIGD2, VDAC1, ZDHHC3, ZNF823

Table 8 Hub genes identified in the PDAC network limited to *mod25* and *mod26*.

Module	GO Term	*p*-value
mod25	endoplasmic reticulum	0.048
mod26	Mitochondrion	0,0077
	Membrane	0,013
	cellular lipid metabolic process	0,017
	transferase activity, transferring acyl groups	0,018
	transmembrane transport	0,021
	hydrolase activity	0,029
	cytoplasmic part	0,039

Table 9 Functional annotation of hub genes in the *mod25* and *mod26*

Module	Transcription factor	*p*-value
mod25	RBPJ	0.0024
	BRCA1	0.0048
	E2F6	0.0100
	E2F1	0.0122
	TCF4	0.0123
	ELK4	0.0126
	FOXA1	0.0127
	CBFB	0.0129
	MIB2	0.0137
	ESR1	0.0144
	SP1	0.0146
	NFIC	0.0156
	HIF1A	0.0169
mod26	FOXO3A	0.0005
	NR1I2	0.0107
	TP63	0.0123

Table 10 Enriched transcription factors binding to the promoters of hub genes

4.3.4 Identification of the hub miRNAs and functional enrichment analysis of their targets

Hub miRNAs, which may play important roles in the PDAC pathogenesis, were identified from the not preserved *M3* and *M4* modules and *Meta-mod* between normal and PDAC networks. The top 20 hub miRNAs identified (Tab. 11) were submitted to the enrichment analysis for the biological and functional interpretation. The hub miRNA list was processed using the miRNet web tool in order to identify enriched KEGG and REACTOME pathways and Gene Ontology (GO) terms (Tab 12, 13 and 14). Genes targeted by the *M3* and *M4* modules were found to be related to cancer pathways, including PDAC and, for the *M3*, to be enriched in genes involved in cell cycle regulation. *Meta-mod* was associated to cancer pathways, apoptosis and transcription regulation.

Module	Hub miRNAs
M3	miR-135a-3p, miR-204-3p, miR-423-5p, miR-575, miR-1343-5p, miR-3918,miR-4419a, miR-4450, miR-4459, miR-4476, miR-4497, miR-4530, miR-4638-5p, miR-4665-5p, miR-4673, miR-6076, miR-6768-5p, miR-6889-5p, miR-6893-5p, miR-6895-5p
M4	miR-302d-3p, miR-382-5p, miR-513c-5p, miR-519c-3p, miR-545-5p, miR-548y, miR-641, miR-873-5p, miR-924, miR-942-3p, miR-1289, miR-2115-3p, miR-3115, miR-3149, miR-3678-5p, miR-4520-2-3p, miR-4527, miR-5007-5p, miR-6866-5p, miR-6882-5p
Meta-mod	miR-196a-3p, miR-548aq-3p, miR-552-5p, miR-890, miR-1269a, miR-1298-3p, miR-2355-3p, miR-4502, miR-4647, miR-4682, miR-4704-5p, miR-4778-5p, miR-4780, miR-6509-5p, miR-6509-3p, miR-6715b-3p, miR-6740-5p, miR-6764-3p, miR-7154-5p, miR-8070

Table 11 Hub miRNAs identified in the PDAC network

Module	Functional annotation
M3 (*p< 0.05*)	Viral carcinogenesis, cell cycle, p53 signaling, bladder cancer, chronic myeloid leukemia, glioma, pancreatic cancer
M4 (*p< 0.01*)	FoxO signaling, p53 signaling, Prostate cancer, Cell cycle, Pancreatic cancer, Chronic myeloid leukemia, Viral carcinogenesis, colorectal cancer, Proteoglycans in cancer, Glioma, Bladder cancer, Hepatitis B, Pathways in cancer
Meta-mod (p< 0.05)	Glioma, chronic myeloid leukemia, ErbB signaling, FoxO signaling non-small cell lung cancer, Wnt signaling, Hippo signaling, pathways in cancer, colorectal cancer

Table 12 Functional annotation of hub miRNAs: enriched KEGG pathways

Module	Functional annotation
M3 (*p< 0.05*)	Pre-NOTCH expression and processing, oncogene induced senescence, cell cycle, mitosis, pre-notch transcription and translation
M4 (*p< 0.001*)	Gene expression, generic transcription pathway, cellular responses to stress,oxidative stress induced senescence, signaling by ERBB4, VEGFR2 mediated vascular permeability, translocation of GLUT4 to the plasma membrane, cellular senescence
Meta-mod (p< 0.05)	Gene expression, activation of BH3-only proteins, intrinsic pathway for apoptosis, membrane trafficking, translocation of GLUT4 to the plasma membrane, vesicle-mediated transport, generic transcription pathway

Table 13 Functional annotation of hub miRNAs: enriched REACTOME pathways

Module	GO biological process	GO molecular function	GO cellular component
M3	None	Purine nucleotide binding, purine ribonucleotide binding, nucleotide binding, ATP binding, adenyl nucleotide binding, adenyl ribonucleotide binding	nucleolus
M4	Regulation of translation	none	none
Meta-Mod	None	Zinc ion binding, chromatin binding, transition metal ion binding.	none

Table 14 Functional annotation of hub miRNAs: enriched ($p < 0.01$) Gene Ontology (GO) terms

4.3.5 Stratification of PDAC patients into high- and low- risk groups based on novel candidate biomarkers

Finally, I evaluated if the lowly preserved modules between the Normal and PDAC datasets (*mod25* and *mod26*) were associated with the overall survival (OS) of PDAC patients [97]. The single-gene and multi-gene survival analyses were performed using the SurvExpress tool on an independent PDAC dataset (GSE21501). I found that the top 20 hub gene from both modules stratified patients into high- and low- risk groups (Fig. 3). The OS of the high-risk group patients was three times shorter than OS of low-risk patients group (HR 3.83 [95 % CI 2.26–6.5] p=6.474e-07 for the *mod25* module and HR 3.41 [95 % CI 1.95–5.85] p=8.813e-06 for the *mod26* module). The single-gene analysis reveals that an increased expression of the CAMKMT (HR 1.76 [95 % CI 1.07–2.89] p=0.02552), PON2 (HR 1.97 [95 % CI 1.19–3.27] p = 0.008798) and SLC25A13 (HR 1.65 [95 % CI 1.01–2.7] p =0.04636) genes was associated with a poor OS. On the contrary, a better OS correlated with the increased expression levels of the following genes: TBC1D24 (HR 1.8 [95 % CI 1.1–2.95] p = 0.02005) and CASK (HR 1.81[95 % CI 1.11–2.96] p = 0.01742).

For the same purpose of validation candidate miRNAs as prognostic biomarkers, single- and multi-miRNA survival analyses in each module (*M3*, *M4* and *Meta-mod*) were performed with the SurvMicro tool, by using the top 20 hub miRNAs as input and an independent miRNA expression dataset of PDAC patients. In all modules, the miRNA profiles stratified PDAC patients into high- and low-risk groups (Fig. 4) and the OS times of the first group were two times shorter compared to the second group (HR 2.79 [95% CI 1.46–5.33] p = 0.001939 for the *M4* module, HR 2.05 [95% CI 1.08–3.89] p = 0.02841 for the *M3* module and HR 2.44 [95% CI 1.28–4.65] p = 0.00645 for the *Meta-mod*). Moreover, the single-miRNA survival analyses were performed to determine miRNA expression alterations significantly associated with PDAC survival outcomes and we found that a better OS was related to an increased expression of miRNAs in Table 15, with the exception of miR-552-5p.

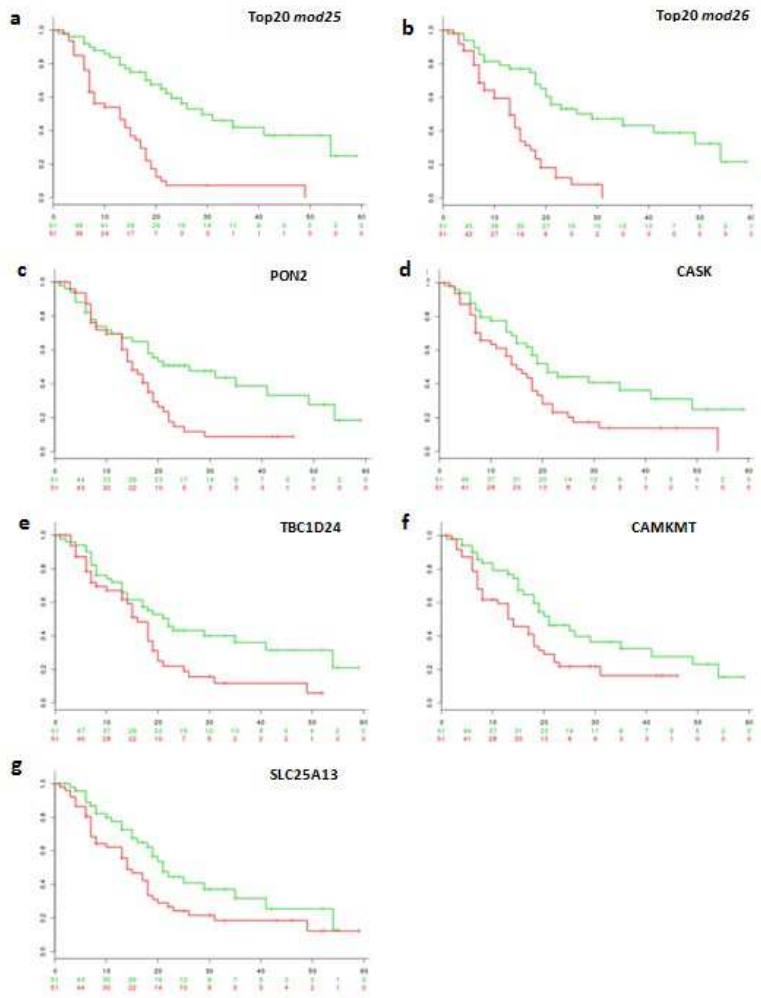

Figure 3 Kaplan-Meier survival plots for OS of (5a and 5b) the top 20 hub gene signatures and of (5c-g) the most significant genes. The X and Y axes respectively stand for survival time (months) and percent of survival people. Red curves represent high-risk group and green curves are low-risk group.

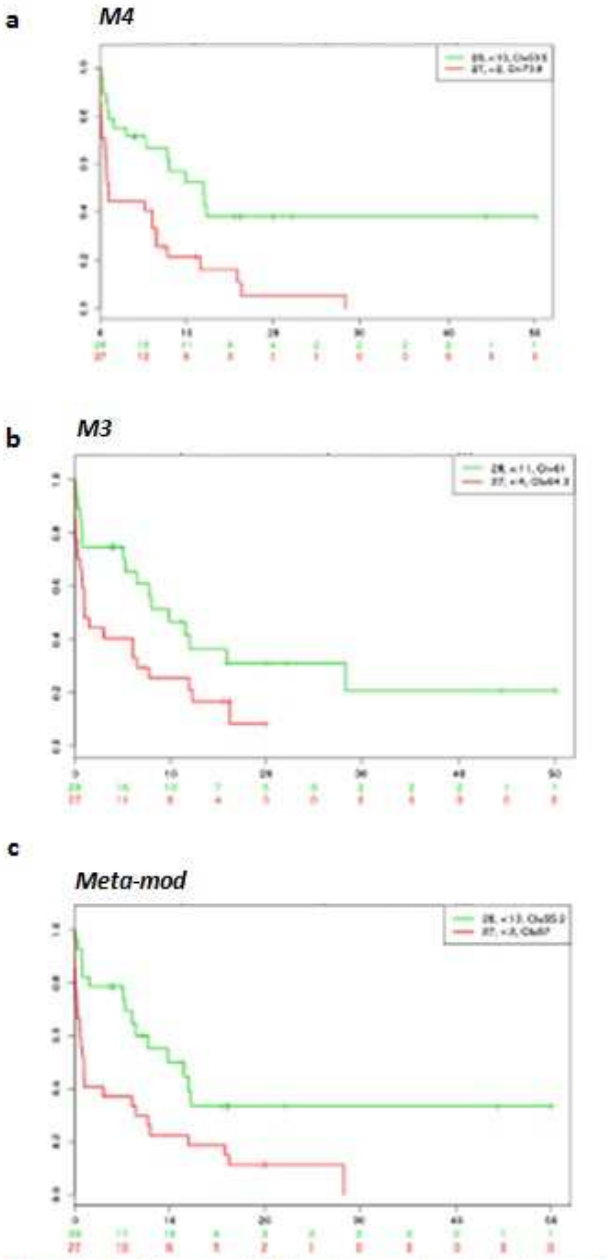

Figure 4 Kaplan-Meier survival plots for overall survival related to (a) the *M4* and (b) *M3* modules and the(c) *Meta-mod* using the top 20 hub miRNA signatures.

Module	Hub miRNA	Hazard Ratio (HR) [Confidence interval 95%]	*p*-value
M3	miR-3918	2,31 [1,22-4,36]	0,01
	miR-575	2,02 [1,08-3,79]	0,0285
M4	miR-3115	2.58 [1.36–4.92]	0,0038
	miR-3149	2.54 [1.33–4.84]	0,0045
	miR-513c-5p	2.27 [1.20–4.29]	0,0114
	miR-519c-3p	2.12 [1.12–4.00]	0,0209
	miR-924	2.02 [1.08–3.79]	0,0285
	miR-548y	2.00 [1.06–3.78]	0,032
	miR-302d-5p	1.95 [1.04–3.69]	0,0387
Meta-mod	miR-1298-3p	2.55 [1.34–4.87]	0,0043
	miR-552-5p	2.34 [1.22–4.50]	0,0105
	miR-890	1.99 [1.05–3.75]	0,0341

Table 15 Single miRNA survival analysis on an independent PDAC miRNA expression dataset

4.4 Discussion

Pancreatic ductal adenocarcinoma (PDAC) urgently needs of identification of new diagnostic and prognostic biomarkers and therapeutic targets. Here we identified, for the first time, candidate genes and microRNAs biomarkers for PDAC by applying weighted gene co-expression network analyses on expression data derived from dataset based on microarrays.

In the first part of the work we focused on gene expression data derived from five datasets based on microarray of PDAC and normal samples. It was found that two modules of co-expressed genes, differed significantly between the Normal and PDAC networks, so they are probably implicated in the pathogenesis. Subsequently, from these two modules I identify the most PDAC-related genes according to WGCNA, i.e. the hub genes. Functional enrichment analysis showed that they are associated to endoplasmatic reticulum (ER), mitochondria, membrane functions, lipid metabolism or transmembrane transport. Regarding genes related to endoplasmatic reticulum, the analyses identified ERLIN2 and TXNDC12 genes. The first has been found to be over-expressed in pancreatic precancerous PanIN-3 cell line [116], whereas the second one inhibited ER stress-induced apoptosis of cancer cells [117]. Moreover, we identified the VDAC1 gene coding for an outer mitochondrial protein presents in a protein complex involved in physical contact between the ER and mitochondria: the mitochondria-associated membrane (MAM). Many protein involved in MAM regulation have been related with cancer [118], indeed VDAC1 protein has been recently found to be over-expressed in PDAC samples [119]. During apoptosis VDAC1 allows the release from mitochondria of CYCS [118], another key factor identified in our work and previously demonstrated to be highly expressed in invasive PDAC [120]. Another hub gene here identified is MCU which codes for a calcium uniporter in the mitochondrial inner membrane. Additional hub genes calcium-related are: CASK, KCNMB3, PON2, SLC25A13 and ZDHHC3. Alteration of the calcium pathway plays a relevant role in PDAC initiation and progression via the Ca2+/calmodulin, PI3Kα/Akt and Raf/MEK/ERK pathways [121, 122] and higher serum calcium level in PDAC patients are associated with a poor prognosis [123]. Various metabolic pathways are altered in cancer cells in order to sustain the abnormal rapid proliferation, among these, lipid synthesis has been observed to be strongly increased [124]. We

determined as hub genes ELOVL6, coding for a fatty acid elongase, NAPEPLD that codes for a lipase, CERS6 and B3GNT5 involved in the ceramide synthesis pathway. Interestingly, among hub genes we found CEACAM1, a member of the carcinoembryonic antigen (CEA) gene family. Previous studies have reported that this gene is more highly expressed in PDAC samples or cell lines [125-127]. Moreover, its protein product, CEA, is currently used as a PDAC biomarker. Through miRNA enrichment analyses I identified miR-202 that, when expressed at low level has been demonstrated to induce apoptosis of PDAC cells. For this reason miR-202 has been proposed as therapeutic target [128]. The chromosomal regions 7q21-q22 and 20q13 identified via chromosomal enrichment analysis may have a role in tumourigenesis since they are already known to be frequently altered in PDAC [129, 130]. The overall survival analyses found that five genes (CAMKMT, CASK, PON2, SLC25A13 and TBC1D24) are associated with a poor OS and they may serve as prognostic biomarker for this cancer.

In the second part, we applied the WGCNA approaches in order to identify circulating miRNA biomarkers and targets through the analysis of microarray-based miRNA expression data obtained from serum of PDAC patients and healthy subjects. We compared networks in normal and PDAC samples and eight out of twelve network modules were found to be not preserved in PDAC network. The potential prognostic value of the miRNAs resulted as hub miRNAs were evaluated in an independent miRNA expression dataset. Through OS analyses we found that the miRNA expression profiles in all modules, and at least two hub miRNAs in each module, were able to effectively discriminate between two distinct prognosis groups. Hub miRNAs belonging to *M4* module mir-942 has previously been found to be over-expressed in PDAC patient serum compared to healthy subjects. miR-302-3p and miR-513 have been upregulated in serum of both PDAC and chronic pancreatitis patients in contrast to healthy donors. Regarding *M3* module, miR-135a-3p is more highly expressed in serum patients than in healthy individuals [131] as well as miR-575 [132]. On the contrary, miR-4497 was found to be down-regulated in serum of PDAC patients compared to healthy subjects [133]. It has been previously described that eight hub miRNAs also found in this module can discriminate PDAC patients from normal subjects: miR-204-3p, miR-423-5p, miR-575, miR-4450, miR-4476, miR-4497, miR-4530 and miR-6893-5p [99]. Among

the hub miRNAs in the *Meta-mod*, miR-196a-3p has not been investigated in PDAC before, but another member of miR-196a family, miR-196a-5p, has widely been detected to be over express in serum PDAC patients [131, 134, 135]. KEEG, REACTOME pathways and GO terms were identified by functional enrichment analysis of hub miRNA target genes. The obtained modules were enriched in PDAC-related pathways and were highly related to cell cycle and gene expression regulation. Finally, we found that many key miRNAs target the hub genes determined above with the same method. For example, the BPNT1, CYCS, MANEAL and SEC23B hub genes are targeted by at least 2 key miRNAs (Tab 16). For this comparison, only experimentally validated miRNA target genes collected by the miRNet tool were used.

Module	Hub miRNAs	Hub genes
M3	miR-3918	CYCS
	miR-4419a	ZDHHC3
	miR-4459	TBC1D24
	miR-4497	BPNT1
	miR-6076	CYCS
	miR-6768-5p	TMEM51
	miR-6893-5p	BPNT1, CYCS
M4	miR-302d-3p	CYCS, MANEAL, SEC23B
	miR-513c-5p	CYCS
	miR-519c-3p	SEC23B
	miR-873-5p	POLDIP2
	miR-924	FLVCR1
	miR-1289	BPNT1
	miR-3149	MANEAL
	miR-6882-5p	MFSD6
Meta-mod	miR-196a-3p	ELOVL6
	miR-548aq-3p	C15ORF52
	miR-4780	MCU

Table 16 Hub genes targeted by hub miRNAs identified by WGCNA. Only experimentally validated miRNA target genes collected by miRNet tool were used for this comparison.

In conclusion, this work identified two modules of co-expressed genes related to pancreatic cancer and new candidate miRNAs as biomarkers. The reliability of our results is confirmed because among our candidate biomarkers we found some genes and miRNAs already suggested as PDAC biomarkers. The results obtained from our

adopted method are different from previously studies performed on single PDAC microarray datasets [23-25] probably because WGCNA seeks hub genes in a co-expression network, differently to the cited works where differentially expressed genes were identified. Moreover, these divergences could be caused by patient variables, such as treatments or disease stage, even if also gender or ethnicity can influence cancer susceptibly or PDAC incidences [136-138]. Unfortunately, this patient information is lacking in the microarray datasets studied until now, so a further analysis and validation of the candidate PDAC biomarkers reported here is necessary. Also, the resulted miRNA biomarkers are needed to be validated by further studies which consider patients information and technical factors, such as blood storage condition and processing.

5. Evaluation of cell death pathways induced by sulforaphane in pancreatic cancer cell lines

5.1. Introduction

5.1.1 Chemoprevention by phytochemicals in pancreatic cancer

Chemoprevention refers to the use of non-toxic natural or synthetic compounds with the capacity to reduce development and progression of cancer. Moderate benefits on the survival extension combined with the undesirable side effects of the standard chemotherapy options have focused recent studies on the anti-tumour effects of plant-derived compounds. Nowadays, nearly 25% of drugs contain active agents from plants and many other promising drugs can be prepared from phytochemicals. Polyphenols, flavonoids, alkaloids, terpenoids and organosulfurs are the principal bioactive agents used against cancer. These compounds act mainly on the cell cycle and apoptotic pathways but there is a risen interest to demonstrate their effects also on non-apoptotic pathways like autophagy, senescence and programmed necrosis [31].

Many epidemiological investigations, during the recent years, have highlighted positive correlations between vegetables, fruits and plant-derived compound consumption and reduced incidence of pancreatic cancer. Numerous studies suggested that bioactive agents inhibit growth and invasiveness of the pancreatic cancer cells *in vitro* and in xenograft models. Phytochemical protagonists of pancreatic cancer prevention and therapy are: curcumin, a commonly food spice isolated from the rhizome of *Curcuma Longa*, capsaicin, that is the pungent element of chilli peppers plants, green tea with its main catechins epigallocatechin-3-gallate (EGCG), resveratrol, detected in many plant species such as red grapes, peanuts, berries and pines, and isothiocynates, secondary metabolites derived from cruciferous vegetables belonging to Brassicacea family [30].

5.1.2 Anti-cancer effects of sulforaphane

The Brassicaceae plant family includes numerous vegetables well known as food products such as broccoli, cabbage, cauliflower and Brussels sprouts. These vegetables contain the inactive glucosinolate glucoraphanin that, when the plant is damaged upon cooking or chewing, is enzymatically hydrolyzed in the active isothiocyanate

sulforaphane [139]. Several works have demonstrated the anti-cancer properties of sulforaphane in human malignancies, including pancreatic cancer, and its limited toxicity in normal tissue. Some epidemiological studies found that frequent consumption of cruciferous vegetables had an about 50% risk reduction to develop pancreatic and prostate cancer [140, 141]. Sulforaphane is involved in different cellular mechanisms that prevent tumour growth. It has been demonstrated in different cancer cell lines that sulforaphane limits the progression of tumour development by causing cell cycle arrest in G2/M phase through the alteration of Cdc2 kinase activity, and by increasing expression of the tumour suppressor and cell cycle inhibitor protein p21. After sulforaphane treatment in colon and prostate cancer cells, the activation of the MAPK/ERK pathway has been reported and it indirectly contributes to cell death. Sulforaphane inhibits cancer cell proliferation by targeting several molecules involved in apoptotic pathways such as Bcl-2, Bax, caspase family, IAP. It has been found that sulforaphane induces apoptosis in cervical HeLa, hepatocellular, prostate and colon cancer cells. It has been reported that incubation of PC3 or HT-29 cells with sulforaphane reduces NF-κB nuclear translocation and results in its transcriptional activity inhibition [32]. NF-κB activation leads its translocation to the nucleus where exerts its central role in cancer cell survival and proliferation by binding to the promoter of many pro-inflammatory genes like inducible nitric oxide synthase (iNOS), cyclooxygenase-2 (COX-2), and tumour necrosis factor (TNF). Recent studies from Kallifatidis et al. (2009, 2011) demonstrated that sulforaphane decreases the enhanced NF-κB activity of apoptosis-resistant pancreatic cancer stem-like cells (CSCs) to basal levels and thereby sensitizes them to chemotherapy-induced apoptosis [142, 143].

5.1.3 Apoptosis and Necroptosis

One of the best-examined forms of cell death is apoptosis, which is initiated by death receptors or mitochondria leading to the activation of two different molecular cascades also known as extrinsic and intrinsic pathways. Both pathways culminate in caspase family member activation that carries out most of the proteolytic processes that occur during apoptosis. Extrinsic pathway begins with the binding of extracellular death ligands (FasL or TNFα) to transmembrane death receptors followed by a complex formation which includes the Fas-associated death domain protein (FADD),

Receptor-Interacting Protein kinase (RIP1) and caspase-8. Activated caspase-8 halts the activities of RIP1 and activates caspase-3 and -7 by proteolytic process [144, 145]. In the intrinsic pathway, stimuli that cause cell stress or damage activate one or more members of the BH3-only protein family. Their activation overcomes the inhibitory effect of the anti-apoptotic B-cell lymphoma-2 (BCL-2) family members facilitating the assembly of BAK–BAX oligomers. These oligomers permit the release from mitochondria of cytochrome *c* which promotes the activation of caspase-9 resulting in further caspase activation events. During apoptosis, cells become rounded, retract from neighbouring cells, and condensation of the nucleus and DNA fragmentation occur. The process culminates in the formation of apoptotic bodies that are readily recognized and phagocytised for recycling of their contents [144].

More recently another form of programmed cell death named necroptosis was identified. It was found that apoptosis-inducing stimuli could mediate cell-death in a caspase-independent manner with morphological features that were similar to necrosis: translucent cytoplasm, cell swelling, organelle dysfunction and rupture of plasma membrane [146]. During the necroptosis induction process, a necrosome complex is formed, with Receptor-Interacting Protein kinase (RIP1), RIP3 and Mixed Lineage Kinase Domain-like Protein (MLKL) as core components. Precisely, RIP1 kinase activity determinates RIP3 phosphorylation which successively phosphorylates and activates MLKL. Then, phosphorylated MLKL translocates to the plasma membrane promoting the necrotic plasma membrane permeabilization. The induction of necroptosis pathway has been proposed as an alternative way to eradicate apoptosis-resistant cancer cells [145, 147].

However, it is not easy to understand apoptosis and necroptosis regulation since components such as RIP1 and RIP3, have been found to contribute to both pathways [148]. RIP1 can induce cell death through the formation of the apoptotic complex RIP1-FADD-caspase-8 or by the activation of RIP3-MLKL necroptotic pathway in response to TNF-stimulated condition [149]. In addition, necroptosis is negatively regulated upon apoptosis induction, since active caspase-8 is known to cleave RIP1 and RIP3 proteolytically [148]. Moreover, the caspase-inhibitor ZVAD, which is routinely used to block apoptosis, was found to induce cell death by necroptosis in a RIP1 and RIP3-

dependent manner in mouse fibrosarcoma cells. In particular, ZVAD promoted autocrine production of TNF through the AP-1 activation [150].

In this study, I have investigated the question whether broccoli-derived isothiocyanate sulforaphane could be involved in induction of both apoptosis and necroptosis, in pancreatic cancer cells. Interestingly, it has been already demonstrated that long-time treatment of pancreatic cancer stem-like cells CSCs with sulforaphane did not induce apoptosis resistance as observed with gemcitabine [151] and it would be interesting to evaluate which is the death pathway involved in the anti-cancer effect of sulforaphane.

5.2. Materials and Methods

5.2.1 Cell culture

The human established PDAC cell line BxPC3 were obtained from the American Type Culture Collection (Manassas, VA, USA). The gemcitabine-resistant subclone BxGEM was established in Herr's lab by continuous gemcitabine treatment in increasing concentrations for more than one year as previously described [151]. The novel cell line of pancreatic ductal adenocarcinoma, originated from intraductal papillarymucinous neoplasm (IPMN), AsanPaca was kindly provided by Dr. N. Giese, Heidelberg [152]. The cells were cultured in DMEM medium (Sigma-Aldrich Chemie, Munich, Germany) supplemented with 10% FCS (Sigma-Aldrich) and 1 mM HEPES (PAA Laboratories Pasching, Austria).

5.2.2 Reagents

D,L-Sulforaphane (Sigma-Aldrich) was dissolved in EtOH to a stock concentration of 50 mM. Caspase inhibitor Z-Val-Ala-DL-Asp(OMe)-fluoromethylketone (ZVAD) was obtained from Bachem (Heidelberg, Germany) and dissolved in DMSO to a stock concentration of 100mM. The necroptosis inhibitor Necrostatin-1s (NECR; BioVision, Milpitas, California, USA) was dissolved in DMSO to 40mM stock solution.

5.2.3. Cell treatments

Cells were grown for 24h to a 50-60% confluence and were treated for 24h with 10 µM D,L-Sulforaphane or 50 µM Zvad or 20 µM Necr-1s. Moreover, pre-treatment for 2h with 50 µM Zvad or 20 µM Necr-1s was performed and then D,L-Sulforaphane was added. Untreated cells and cells treated with vehicles (DMSO 1:2000; EtOH 1:5000; DMSO 1:2000+ EtOH 1:5000) were used as control groups.

5.2.4 Cell viability detection by MTT assay

BxPC3 and BxGEM were seeded at a density of 4 x 10^3 and AsanPaca 5 x 10^3 in 96-well microplates, 100 µl per well. After treatment, cell viability was measured adding 10 µl in each well of 12mM MTT-solution (3-(4,5-dimethylthiazol-2-yl)-2,5-diphenyltetrazolium bromide; Sigma-Aldrich) followed by incubation at 37°C for 3h. Medium was replaced by 200 µl dimethyl sulphoxide and, after short incubation under shaking, the optical density of wells, was measured by FLUOstar® Omega microplate reader at 550 nm wavelength [153].

5.2.5 Detection of apoptosis by Annexin V/PI staining and FACS analysis

Cells were grown in 6-well plates (BxPC3 and BxGEM: 8 x 10^4 cells per well; AsanPaca: 1 x 10^5). After treatment cells were detached with 500 µl/well of Accutase (Sigma-Aldrich), in order to preserve cell surface markers, collected and resuspended in 500 µl Annexin Binding Buffer 1x (eBioscience, San Diego, California, USA). Then, cells were transferred in 96-well plate (100 µl each treatment groups) and stained with 5 µl FITC-conjugated Annexin-V (eBioscience). After 15 minutes of incubation at room temperature in the dark and washing with Binding Buffer, resuspended single-cells were moved in FACS tubes. Two microlitres of Propidium Iodide (BD Biosciences, Heidelberg, Germany) were added in every tube only five minutes before measurements to preserve cells from its strong action. Cells were analysed with a BD FACS Canto flow cytometer and FlowJo software (both from BD Biosciences, Heidelberg, Germany).

5.2.6 Detection of active caspase-3 by immunocytochemistry

Cells were treated for 24h as described above, were cytospinned to glass slides and fixed with 4% paraformaldehyde for 10 minutes. After the blocking phase with 20% goat serum in PBS for 30 minutes, the expression of active fragment of caspase-3 was examined by binding with a specific antibody (R&D System, Minneapolis, Minnesota, USA) for 1h. Endogenous peroxidase activity was blocked with 0.03% hydrogen peroxide. The binding of primary antibody was detected using goat anti-rabbit biotinylated IgG (Vector Laboratories, Burlingame, California, USA) served as secondary antibody. The signal was amplified with the ABC kit (Vector Laboratories, Burlingame, California, USA), AEC Single Solution (Zytomed system, Berlin, Germany) was used as a chromogen and haematoxylin was used as counterstain. Washing steps were performed two times with PBS-Tween and one time with PBS. The omission of the primary antibody was used as a negative control.

5.2.7 Cell lysis and determination of protein concentration

After treatment, cells grown on petri dishes were lysed by adding 100-200 µl of membrane extraction buffer (30 mM Tris pH 7,4; 150 mM NaCl; 1 mM EDTA; 0,5 % Triton-X-100; 0,5% Na-Deoxycholate) supplemented with phosphatase and protease inhibitors for 5 minutes on ice. The cells were scraped from the plates and the volume

collected was transferred to 1,5 ml tubes. After centrifugation at higher speed for 15 min at 4°C the supernatant was transferred into new tubes. For quantification of protein concentration Pierce BCA Protein Assay kit (Thermo Scientific) was used. BSA standards and BCA working agent were prepared according to the manufacturer's instructions. Then, 10 µl of each BSA standard or 5 µl of proteins samples were added in 96-well plate followed by 200 µl/well of BCA working agent. After 30 minutes at 37°C incubation, the absorbance at 562 nm was measured with FLUOstar® Omega microplate reader. Protein solutions were diluted 1:3 with Laemmli buffer 4x, boiled at 99°C for 3 minutes and incubated on ice. Standard curve was used to calculate the volume to load in order to have the same amount of protein for each sample.

5.2.8 Detection of RIP1 and MLKL by Western blot analysis

Denatured proteins were loaded on stacking gel (4% acrylamide) and separated electrophoretically on a 12% polyacrylamid gel according to their molecular weight. PageRuler™ Prestained Protein Ladder (ThermoFisher), 5 µl, was loaded as size standard. The gel was fixed in a gel chamber filled with SDS-running buffer 1x pH 8.3 (192 mM Glycine; SDS 0.1%; 25 mM Tris). Migration through stacking gel was performed at 80V for 20 minutes followed by separation at 160V for 1h. Separated proteins were then transferred on Immobilon-FL PVDF transfer membrane (Merck Millipore, Darmstadt, Germany), previously activated with 100% methanol. The semi-dry transfer was performed preparing a sandwich of membrane and gel, enclosed in filter papers wet in transfer buffer (39 mM Glycine; 48 mM Tris, SDS 0.0375%; Methanol 20%) for 90 minutes at 0.06 A. After blocking with 5% BSA/TBS-T, the following primary antibodies were used: mouse IgG2a anti-RIP1 (BD Bioscience, Heidelberg, Germany), rabbit polyclonal anti-MLKL (Novus Biological) were incubated overnight and β-actin (Sigma-Aldrich, Munich, Germany) was incubated for 30 minutes. After three washes with 5% BSA/TBS-T, anti-mouse and anti-rabbit-IgG, IRDye® 800CW or 680RD Infrared Dye (LI-COR Biosciences, Bad Homburg, Germany) were used as secondary antibodies for a 30 minutes incubation. The membrane exposure was carried out in a LI-COR Biosciences Odyssey infrared imaging system machine. The intensity of protein signal was determined by ImageJ software (https://imagej.nih.gov/ij/).

5.2.9 Statistical analysis

The MTT assay was performed in eight replicates (n=8). The significance of the data was analyzed with a t-test corrected for multiple testing. Annexin/PI assays were performed in three independent experiment (n=3). For BxPC3 and BxGEM cells, the differences between groups were calculated with a t-test corrected for multiple testing by the Bonferroni-Holm method. In the AsanPaca cell line, one replicate was refused and the Mann-Whitney-U test was used instead of the t-test. Regarding immunocytochemistry, the number of positive cells was counted in 100 vision fields for each treatment group. The significance of the data was analysed with unpaired t-test by GraphPad Prism 7. The data are presented as the means ±SEM. $p<0.05$ was considered statistically significant (*) and $p<0.01$ was considered highly significant (**).

5.3. Results

5.3.1 Sulforaphane-reduced viability involves caspases, whereas necroptosis plays a minor role

To assess whether sulforaphane induces apoptosis and/or necroptosis, three PDAC cells lines, BxPC3, BxGEM and AsanPaCa, were treated with the bioactive agent, for 24h, alone or in combination with specific inhibitors. In particular, the pan-caspase inhibitor ZVAD was used to explore whether sulforaphane can trigger necroptosis when the caspase activation and apoptosis are blocked. NECR was used to inhibit the kinase activity of RIP1, preventing the RIP1/RIP3 interaction and blocking necrosis [154, 155]. Whereas BxPC3 and AsanPaCa are sensitive to gemcitabine-treatment, BxGEM cells are not, because this drug-resistant subclone has been selected by continuous gemcitabine treatment and acquired apoptosis resistance [151]. Thus, it may be expected that defective apoptosis is compensated by necroptosis.

Toxicity of single treatments or their combination was determined by the MTT assay (Fig. 5). Whereas vehicle controls ZVAD and NECR alone did not diminish viability, sulforaphane reduces it in BxPC3 and BxGEM cells to 40% and 38%, respectively, while a slight effect was observed in AsanPaCa with 23% mortality. On the contrary, the pre-treatment with ZVAD 2h before the sulforaphane addition reduced the mortality, particularly in BxGEM cells. As expected, a minor effect on sulforaphane-mediated mortality by NECR pre-treatment was observed.

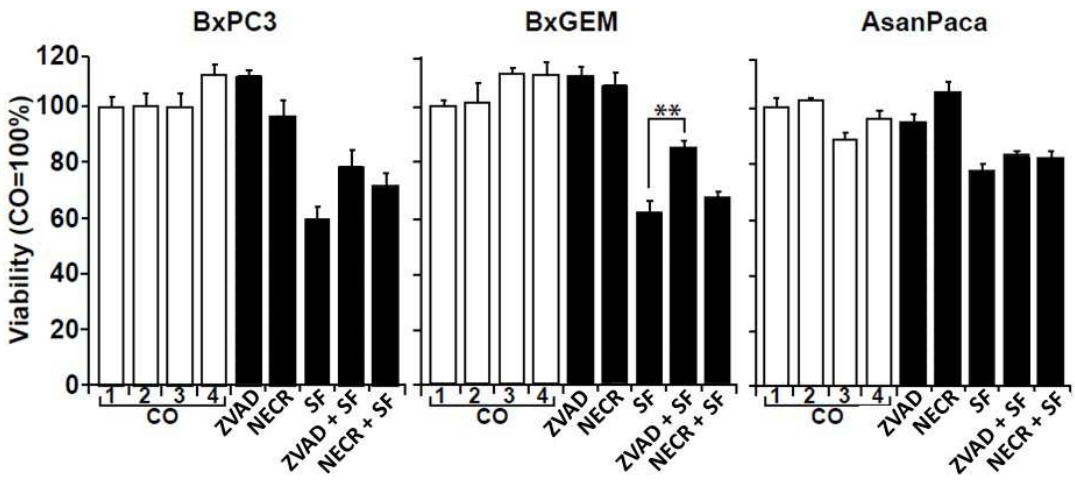

Figure 5 MTT assay. BxPC3, BxGEM and AsanPaca were left untreated, or were treated for 24h with vehicle (1: CO; 2: DMSO 1:2000; 3: EtOH 1:5000; 4: DMSO 1:2000+ EtOH 1:5000) or with SF (10 μM), ZVAD (50 μM), NECR (20 μM) or the pre-treatment for 2h with the inhibitors was followed by SF addition. The cells viability was detected after 24h. The percentage of viable cells in the CO group was set to 100%, data are presented as the means ±SEM.**P<0.01

5.3.2 Sulforaphane-induced cell death involves caspases

To further examine if sulforaphane induces both, apoptosis or necroptosis, cells were treated as described in the Materials and Methods section, and 24h later were stained with Annexin V and propidium iodide followed by FACS analysis. Annexin V protein binds to phosphatidylserine expressed on the apoptotic cells surface before the loss of plasma membrane integrity while propidium iodide binds DNA, but it is not membrane-permeable, and therefore its positivity is a necrosis or late apoptosis index [156]. FACS analysis showed that sulforaphane increased the percentage of early apoptotic cells and induced a much higher percentage of the double positive cells indicating late apoptosis or necrosis. Interestingly, ZVAD pre-treatment almost completely impeded sulforaphane-induced apoptosis, with statistically significant results in BxGEM. Pre-treatment with NECR had a small effect on the cell death induction by sulforaphane in BxPC3, whereas it prevented sulforaphane-induced apoptosis in BxGEM cells. A similar tendency was observed among the different treatment groups in AsanPaca, too, but in this case sulforaphane had a mild effect (Fig. 6). These results show that the toxic effect of sulforaphane is completely blocked when caspases are inhibited by ZVAD, and the low percentages of cell-death indicate that

sulforaphane does not trigger necroptosis. The bioactive agent sulforaphane induces cell death only in a caspase-dependent manner.

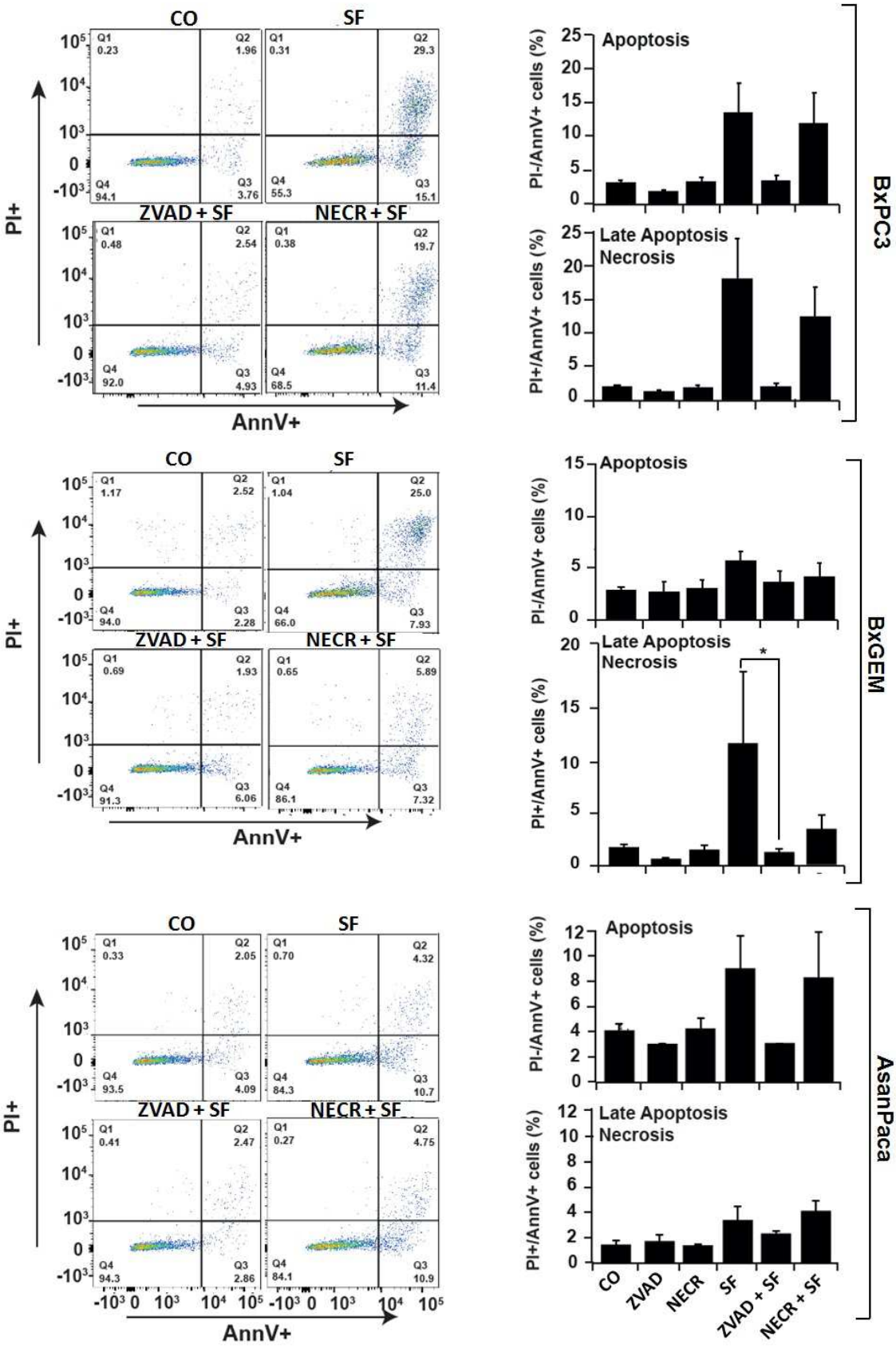

Figure 6 Annexin V/PI assay. BxPC3, BxGEM and AsanPaca were treated for 24h as previously described. Q1: necrosis ($Annexin^-/PI^+$); Q2: late apoptosis/necrosis ($Annexin^+/PI^+$); Q3: apoptosis ($Annexin^+/PI^-$); Q4: live cells ($Annexin^-/PI^-$). The percentages of apoptotic and late apoptotic/necrotic cells are shown as the means ±SEM. The outcomes from untreated cells and from all the vehicles controls (DMSO 1:2000; EtOH 1:5000; DMSO 1:2000+ EtOH 1:5000) were pooled and the means ±SEM is shown in the diagram as CO. *P<0.05.

5.3.3 Sulforaphane-induced caspase-3 cleavage

Successively, the expression level of the cleaved fragment of active caspase-3 was analysed by immunocytochemistry on the three cell lines, previously cytospinned to glass slides. Positive cells were evaluated by counting of 100 vision fields. As expected, the percentage of positive cells was greater upon treatment with sulforaphane and NECR pre-treatment compared to the control group, while ZVAD pre-treatment totally blocked sulforaphane-induced caspase-3 cleavage (Fig. 7).

5.3.4 Sulforaphane reduces RIP1 and MLKL protein expression

I focused on the protein levels of RIP1 and MLKL, two essential components of the necrosome complex [145], in order to confirm that necroptosis was not involved in sulforaphane-induced cell death. BxPC3 cells were treated as described above, followed by extraction of whole cell proteins 24h later and western blot analysis.

In examining the protein level of RIP1 upon sulforaphane treatment, I observed a weaker band compared to control band. This last could represent the phosphorylated form of RIP1 [157] leading me to conclude that sulforaphane prevents RIP1 phosphorylation and thus its activation. As expected, ZVAD pre-treatment prevents sulforaphane effect. As shown in a previous work, NECR treatment decreased RIP1 phosphorylation [158] but my work shows that the combination of NECR and sulforaphane treatment lead to decrease of RIP1 protein expression. In the Figure 8 it is possible to observe that protein expression of MLKL, the functional substrate for RIP3 kinase [147], depends on RIP1 phosphorylation.

These findings suggest that the broccoli-derived agent sulforaphane induces apoptosis at 10 μM concentration and prevents the necrosome activation.

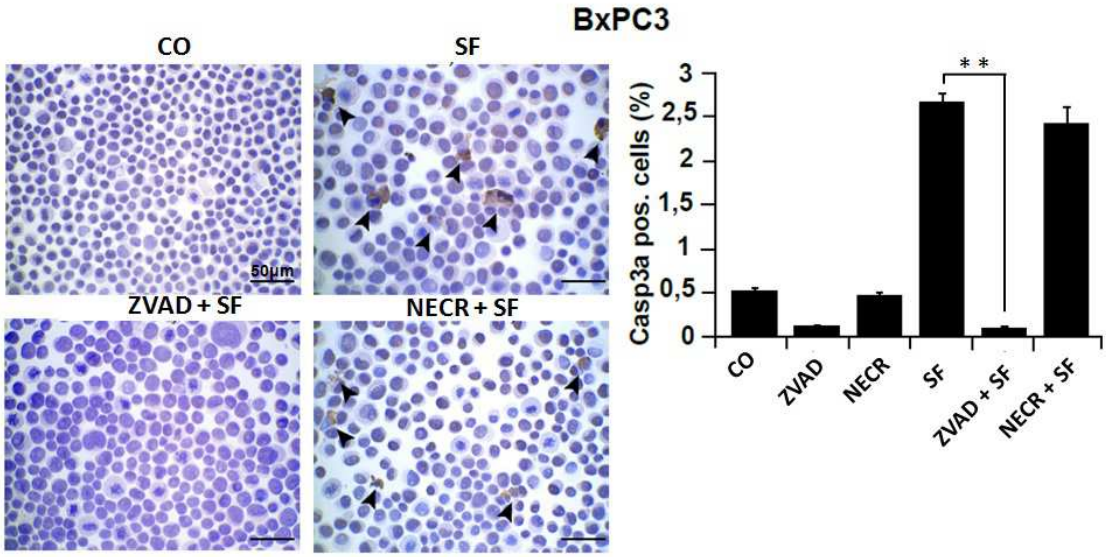
BxPC3
CO
SF
50µm
ZVAD + SF
NECR + SF
Casp3a pos. cells (%)
3
2,5
2
1,5
1
0,5
0
* *
CO
ZVAD
NECR
SF
ZVAD + SF
NECR + SF

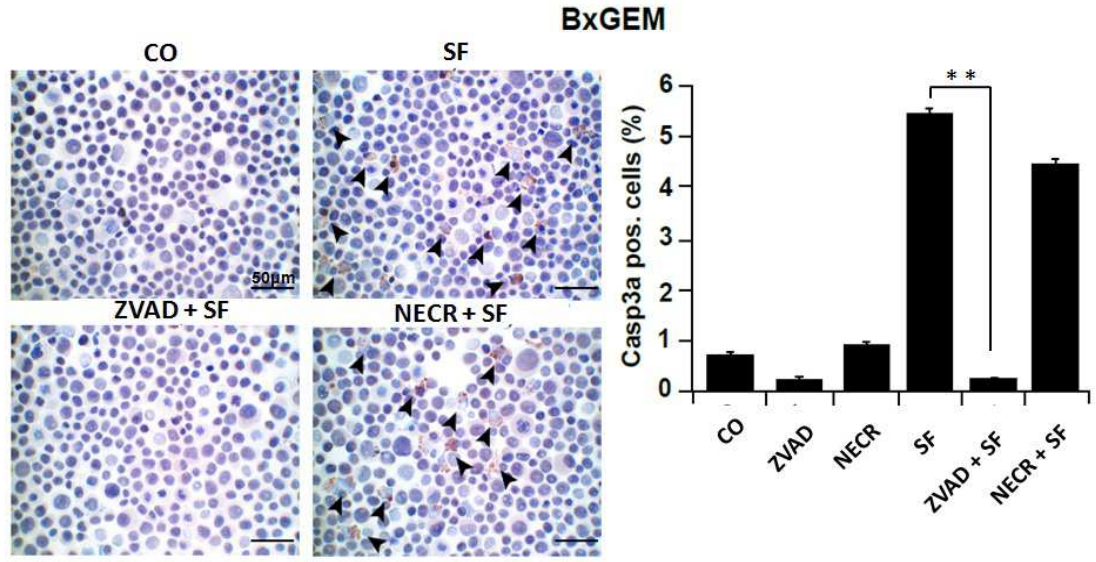
BxGEM
CO
SF
50µm
ZVAD + SF
NECR + SF
Casp3a pos. cells (%)
6
5
4
3
2
1
0
* *
CO
ZVAD
NECR
SF
ZVAD + SF
NECR + SF

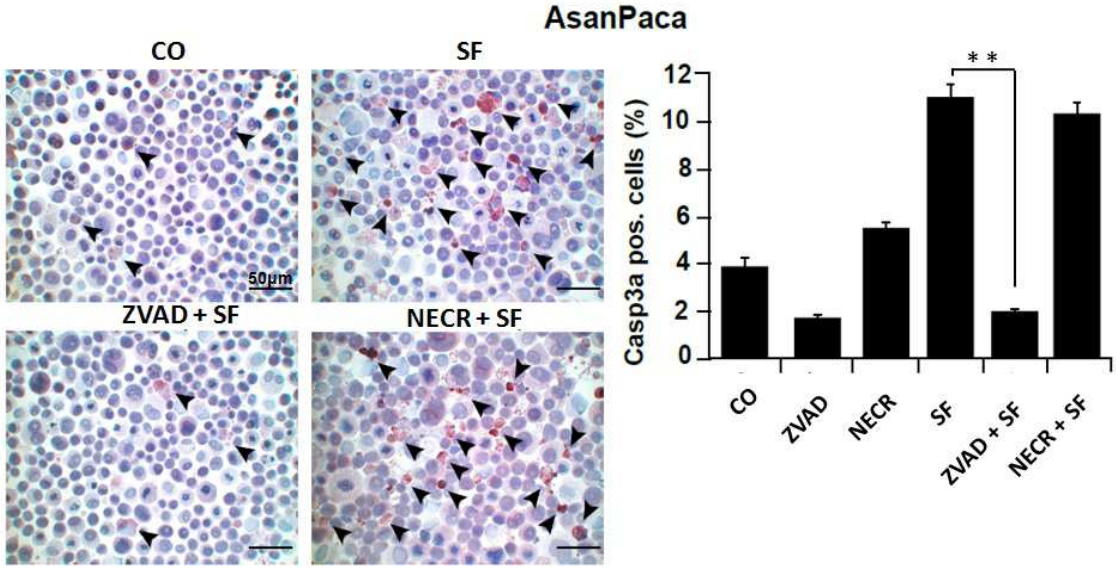
AsanPaca
CO
SF
50µm
ZVAD + SF
NECR + SF
Casp3a pos. cells (%)
12
10
8
6
4
2
0
* *
CO
ZVAD
NECR
SF
ZVAD + SF
NECR + SF

Figure 7 Immunocytochemistry. BxPC3, BxGEM and AsanPaca. Twenty-four hours later the cells were cytospinned to glass slides and the active fragment of Caspase-3 was examined at a magnification of x40. Black arrows indicate the positive cells. The number of positive cells was counted in 100 vision fields and the means ± SEM are shown in the diagrams. ** means P<0.01

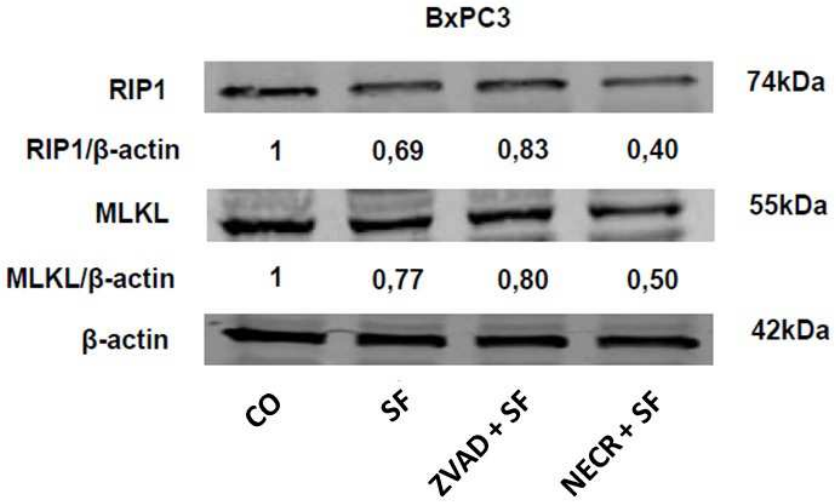

Figure 8 Western Blot. BxPC3 cells were left untreated (CO), or treated as previously described. After 24h the protein extracts were prepared. 40 μg of protein was loaded on the gels and the expression of RIP1 and MLKL was detected. β-Actin served as internal loading control. The intensity of the signal of each protein was determined by ImageJ software (downloaded from the NIH website (http://rsb.info.nih.gov/ij)).

5.4. Discussion

I evaluated the effect of the phytochemical sulforaphane on the apoptosis and necroptosis induction in pancreatic cancer cells.

Sulforaphane is a promising anti-cancer substance with well documented antioxidant, chemopreventative, and anti-tumour properties. Previous data from Kallifatidis (2009) showed the apoptotic effect of sulforaphane on highly treatment-resistant tumour-initiating cells in pancreatic carcinoma [159]. Moreover, sulforaphane had no toxic effects on normal cells and, importantly, did not induce drug resistance in pancreatic cancer cells [151] but enhanced chemotherapeutic agents effect [160-162]. Here I have examined whether sulforaphane-induced cell death is mediated by necroptosis in a situation of blocked apoptosis, and *vice-versa*. I used the gemcitabine-resistant subclone BxGEM with acquired apoptosis resistance, the parental cell clone BxPC3, and the novel cell line of pancreatic ductal adenocarcinoma, originated from IPMN, AsanPaca. The apoptosis signalling was blocked by ZVAD, and likewise necroptosis was blocked by the RIP1 inhibitor NECR. By examination of cell viability, I have assessed that ZVAD partially reversed sulforaphane-reduced viability, with significant effects in BxGEM cells, whereas NECR had instead no effects. These results suggest that sulforaphane requires caspases for induction of cell death as well as demonstrated by the FACS measurements. It has been shown that ZVAD was able to prevent sulforaphane-induced apoptosis in all cell lines, whereas in BxGEM cells, also NECR was able to prevent late apoptosis/necrosis. This may be due to the inability of BxGEM cells to switch to apoptosis in a situation of blocked necrosis, due to an acquired apoptosis defect in this particular cell line [151].

In the recent years, numerous studies showed that necroptosis could be induced by pan-caspase inhibitors in combination with chemotherapeutic agents such as 5-FU, or with the smac-mimetic BV6 or with TNF or with staurosporine, in different cancer cell lines that are resistant to pro-apoptotic treatments [163-165]. However, data in the present study indicate that the combination of pan-caspase inhibitor and sulforaphane does not lead to necroptosis-induced cell death. The bioactive agent cannot completely exert its toxic effect on pancreatic cells with Zvad co-treatment. In fact, cell viability is rescued and the percentages of apoptotic cells are comparable to the control group (Fig. 5, 6). Moreover, immunohistochemistry results confirmed that

sulforaphane induces apoptosis (Fig. 7) and seems to have an inhibitor effect on the RIP1 phosphorylation with consequences on necrosome complex activation (Fig. 8). These results suggest that probably sulforaphane does not trigger the necroptotic pathway, but may help caspase-8 to exert the apoptotic cascade. However, more detailed analyses are required in the future studies.

6 References

1 Rahib L, Smith BD, Aizenberg R, Rosenzweig AB, Fleshman JM, Matrisian LM: Projecting cancer incidence and deaths to 2030: The unexpected burden of thyroid, liver, and pancreas cancers in the united states. Cancer Res 2014;74:2913-2921.

2 Malvezzi M, Carioli G, Bertuccio P, Rosso T, Boffetta P, Levi F, La Vecchia C, Negri E: European cancer mortality predictions for the year 2016 with focus on leukaemias. Ann Oncol 2016;27:725-731.

3 Kleeff J, Korc M, Apte M, La Vecchia C, Johnson CD, Biankin AV, Neale RE, Tempero M, Tuveson DA, Hruban RH, Neoptolemos JP: Pancreatic cancer. Nat Rev Dis Primers 2016;2:16022.

4 Wolfgang CL, Herman JM, Laheru DA, Klein AP, Erdek MA, Fishman EK, Hruban RH: Recent progress in pancreatic cancer. CA Cancer J Clin 2013;63:318-348.

5 Arslan AA, Helzlsouer KJ, Kooperberg C, Shu XO, Steplowski E, Bueno-de-Mesquita HB, Fuchs CS, Gross MD, Jacobs EJ, Lacroix AZ, Petersen GM, Stolzenberg-Solomon RZ, Zheng W, Albanes D, Amundadottir L, Bamlet WR, Barricarte A, Bingham SA, Boeing H, Boutron-Ruault MC, Buring JE, Chanock SJ, Clipp S, Gaziano JM, Giovannucci EL, Hankinson SE, Hartge P, Hoover RN, Hunter DJ, Hutchinson A, Jacobs KB, Kraft P, Lynch SM, Manjer J, Manson JE, McTiernan A, McWilliams RR, Mendelsohn JB, Michaud DS, Palli D, Rohan TE, Slimani N, Thomas G, Tjonneland A, Tobias GS, Trichopoulos D, Virtamo J, Wolpin BM, Yu K, Zeleniuch-Jacquotte A, Patel AV: Anthropometric measures, body mass index, and pancreatic cancer: A pooled analysis from the pancreatic cancer cohort consortium (panscan). Arch Intern Med 2010;170:791-802.

6 Bosetti C, Rosato V, Li D, Silverman D, Petersen GM, Bracci PM, Neale RE, Muscat J, Anderson K, Gallinger S, Olson SH, Miller AB, Bas Bueno-de-Mesquita H, Scelo G, Janout V, Holcatova I, Lagiou P, Serraino D, Lucenteforte E, Fabianova E, Ghadirian P, Baghurst PA, Zatonski W, Foretova L, Fontham E, Bamlet WR, Holly EA, Negri E, Hassan M, Prizment A, Cotterchio M, Cleary S, Kurtz RC, Maisonneuve P, Trichopoulos D, Polesel J, Duell EJ, Boffetta P, La Vecchia C: Diabetes, antidiabetic medications, and pancreatic cancer risk: An analysis from the international pancreatic cancer case-control consortium. Ann Oncol 2014;25:2065-2072.

7 Kamisawa T, Wood LD, Itoi T, Takaori K: Pancreatic cancer. Lancet 2016;388:73-85.

8 Scarpa A, Chang DK, Nones K, Corbo V, Patch AM, Bailey P, Lawlor RT, Johns AL, Miller DK, Mafficini A, Rusev B, Scardoni M, Antonello D, Barbi S, Sikora KO, Cingarlini S, Vicentini C, McKay S, Quinn MC, Bruxner TJ, Christ AN, Harliwong I, Idrisoglu S, McLean S, Nourse C, Nourbakhsh E, Wilson PJ, Anderson MJ, Fink JL, Newell F, Waddell N, Holmes O, Kazakoff SH, Leonard C, Wood S, Xu Q, Nagaraj SH, Amato E, Dalai I, Bersani S, Cataldo I, Dei Tos AP, Capelli P, Davi MV, Landoni L, Malpaga A, Miotto M, Whitehall VL, Leggett BA, Harris JL, Harris J, Jones MD, Humphris J, Chantrill LA, Chin V, Nagrial AM, Pajic M, Scarlett CJ, Pinho A, Rooman I, Toon C, Wu J, Pinese M, Cowley M, Barbour A, Mawson A, Humphrey ES, Colvin EK, Chou A, Lovell JA, Jamieson NB, Duthie F, Gingras MC, Fisher WE, Dagg RA, Lau LM, Lee M, Pickett HA, Reddel RR, Samra JS, Kench JG, Merrett ND, Epari K, Nguyen NQ, Zeps N, Falconi M, Simbolo M, Butturini G, Van Buren G, Partelli S, Fassan M, Khanna KK, Gill AJ, Wheeler DA, Gibbs RA, Musgrove EA, Bassi C, Tortora G, Pederzoli P, Pearson JV, Biankin AV, Grimmond SM: Whole-genome landscape of pancreatic neuroendocrine tumours. Nature 2017;543:65-71.

9 Low G, Panu A, Millo N, Leen E: Multimodality imaging of neoplastic and nonneoplastic solid lesions of the pancreas. Radiographics 2011;31:993-1015.

10 Delpu Y, Hanoun N, Lulka H, Sicard F, Selves J, Buscail L, Torrisani J, Cordelier P: Genetic and epigenetic alterations in pancreatic carcinogenesis. Curr Genomics 2011;12:15-24.

11 Pandol S, Edderkaoui M, Gukovsky I, Lugea A, Gukovskaya A: Desmoplasia of pancreatic ductal adenocarcinoma. Clin Gastroenterol Hepatol 2009;7:S44-47.

12 Patel MB, Pothula SP, Xu Z, Lee AK, Goldstein D, Pirola RC, Apte MV, Wilson JS: The role of the hepatocyte growth factor/c-met pathway in pancreatic stellate cell-endothelial cell interactions: Antiangiogenic implications in pancreatic cancer. Carcinogenesis 2014;35:1891-1900.
13 Hamada S, Masamune A, Takikawa T, Suzuki N, Kikuta K, Hirota M, Hamada H, Kobune M, Satoh K, Shimosegawa T: Pancreatic stellate cells enhance stem cell-like phenotypes in pancreatic cancer cells. Biochem Biophys Res Commun 2012;421:349-354.
14 Xu Z, Vonlaufen A, Phillips PA, Fiala-Beer E, Zhang X, Yang L, Biankin AV, Goldstein D, Pirola RC, Wilson JS, Apte MV: Role of pancreatic stellate cells in pancreatic cancer metastasis. Am J Pathol 2010;177:2585-2596.
15 Nielsen MF, Mortensen MB, Detlefsen S: Key players in pancreatic cancer-stroma interaction: Cancer-associated fibroblasts, endothelial and inflammatory cells. World J Gastroenterol 2016;22:2678-2700.
16 Lambert AW, Pattabiraman DR, Weinberg RA: Emerging biological principles of metastasis. Cell 2017;168:670-691.
17 Costa-Silva B, Aiello NM, Ocean AJ, Singh S, Zhang H, Thakur BK, Becker A, Hoshino A, Mark MT, Molina H, Xiang J, Zhang T, Theilen TM, Garcia-Santos G, Williams C, Ararso Y, Huang Y, Rodrigues G, Shen TL, Labori KJ, Lothe IM, Kure EH, Hernandez J, Doussot A, Ebbesen SH, Grandgenett PM, Hollingsworth MA, Jain M, Mallya K, Batra SK, Jarnagin WR, Schwartz RE, Matei I, Peinado H, Stanger BZ, Bromberg J, Lyden D: Pancreatic cancer exosomes initiate pre-metastatic niche formation in the liver. Nat Cell Biol 2015;17:816-826.
18 Bettegowda C, Sausen M, Leary RJ, Kinde I, Wang Y, Agrawal N, Bartlett BR, Wang H, Luber B, Alani RM, Antonarakis ES, Azad NS, Bardelli A, Brem H, Cameron JL, Lee CC, Fecher LA, Gallia GL, Gibbs P, Le D, Giuntoli RL, Goggins M, Hogarty MD, Holdhoff M, Hong SM, Jiao Y, Juhl HH, Kim JJ, Siravegna G, Laheru DA, Lauricella C, Lim M, Lipson EJ, Marie SK, Netto GJ, Oliner KS, Olivi A, Olsson L, Riggins GJ, Sartore-Bianchi A, Schmidt K, Shih l M, Oba-Shinjo SM, Siena S, Theodorescu D, Tie J, Harkins TT, Veronese S, Wang TL, Weingart JD, Wolfgang CL, Wood LD, Xing D, Hruban RH, Wu J, Allen PJ, Schmidt CM, Choti MA, Velculescu VE, Kinzler KW, Vogelstein B, Papadopoulos N, Diaz LA, Jr.: Detection of circulating tumor DNA in early- and late-stage human malignancies. Sci Transl Med 2014;6:224ra224.
19 Majumder S, Chari ST, Ahlquist DA: Molecular detection of pancreatic neoplasia: Current status and future promise. World J Gastroenterol 2015;21:11387-11395.
20 Sausen M, Phallen J, Adleff V, Jones S, Leary RJ, Barrett MT, Anagnostou V, Parpart-Li S, Murphy D, Kay Li Q, Hruban CA, Scharpf R, White JR, O'Dwyer PJ, Allen PJ, Eshleman JR, Thompson CB, Klimstra DS, Linehan DC, Maitra A, Hruban RH, Diaz LA, Jr., Von Hoff DD, Johansen JS, Drebin JA, Velculescu VE: Clinical implications of genomic alterations in the tumour and circulation of pancreatic cancer patients. Nat Commun 2015;6:7686.
21 Melo SA, Luecke LB, Kahlert C, Fernandez AF, Gammon ST, Kaye J, LeBleu VS, Mittendorf EA, Weitz J, Rahbari N, Reissfelder C, Pilarsky C, Fraga MF, Piwnica-Worms D, Kalluri R: Glypican-1 identifies cancer exosomes and detects early pancreatic cancer. Nature 2015;523:177-182.
22 Occhipinti G, Giulietti M, Principato G, Piva F: The choice of endogenous controls in exosomal microrna assessments from biofluids. Tumour Biol 2016;37:11657-11665.
23 Badea L, Herlea V, Dima SO, Dumitrascu T, Popescu I: Combined gene expression analysis of whole-tissue and microdissected pancreatic ductal adenocarcinoma identifies genes specifically overexpressed in tumor epithelia. Hepatogastroenterology 2008;55:2016-2027.
24 Donahue TR, Tran LM, Hill R, Li Y, Kovochich A, Calvopina JH, Patel SG, Wu N, Hindoyan A, Farrell JJ, Li X, Dawson DW, Wu H: Integrative survival-based molecular profiling of human pancreatic cancer. Clin Cancer Res 2012;18:1352-1363.
25 Zhang G, Schetter A, He P, Funamizu N, Gaedcke J, Ghadimi BM, Ried T, Hassan R, Yfantis HG, Lee DH, Lacy C, Maitra A, Hanna N, Alexander HR, Hussain SP: Dpep1 inhibits tumor

cell invasiveness, enhances chemosensitivity and predicts clinical outcome in pancreatic ductal adenocarcinoma. PLoS One 2012;7:e31507.
26 Giulietti M, Occhipinti G, Principato G, Piva F: Weighted gene co-expression network analysis reveals key genes involved in pancreatic ductal adenocarcinoma development. Cell Oncol (Dordr) 2016;39:379-388.
27 Giulietti M, Occhipinti G, Principato G, Piva F: Identification of candidate mirna biomarkers for pancreatic ductal adenocarcinoma by weighted gene co-expression network analysis. Cell Oncol (Dordr) 2017;40:181-192.
28 Hidalgo M, Cascinu S, Kleeff J, Labianca R, Lohr JM, Neoptolemos J, Real FX, Van Laethem JL, Heinemann V: Addressing the challenges of pancreatic cancer: Future directions for improving outcomes. Pancreatology 2015;15:8-18.
29 Chiaravalli M, Reni M, O'Reilly EM: Pancreatic ductal adenocarcinoma: State-of-the-art 2017 and new therapeutic strategies. Cancer Treat Rev 2017;60:32-43.
30 Boreddy SR, Srivastava SK: Pancreatic cancer chemoprevention by phytochemicals. Cancer Lett 2013;334:86-94.
31 Gali-Muhtasib H, Hmadi R, Kareh M, Tohme R, Darwiche N: Cell death mechanisms of plant-derived anticancer drugs: Beyond apoptosis. Apoptosis 2015;20:1531-1562.
32 Tortorella SM, Royce SG, Licciardi PV, Karagiannis TC: Dietary sulforaphane in cancer chemoprevention: The role of epigenetic regulation and hdac inhibition. Antioxid Redox Signal 2015;22:1382-1424.
33 Kharaziha P, Ceder S, Li Q, Panaretakis T: Tumor cell-derived exosomes: A message in a bottle. Biochim Biophys Acta 2012;1826:103-111.
34 Muralidharan-Chari V, Clancy JW, Sedgwick A, D'Souza-Schorey C: Microvesicles: Mediators of extracellular communication during cancer progression. J Cell Sci 2010;123:1603-1611.
35 Johnstone RM, Adam M, Hammond JR, Orr L, Turbide C: Vesicle formation during reticulocyte maturation. Association of plasma membrane activities with released vesicles (exosomes). J Biol Chem 1987;262:9412-9420.
36 Kowal J, Tkach M, Thery C: Biogenesis and secretion of exosomes. Curr Opin Cell Biol 2014;29:116-125.
37 Valadi H, Ekstrom K, Bossios A, Sjostrand M, Lee JJ, Lotvall JO: Exosome-mediated transfer of mrnas and micrornas is a novel mechanism of genetic exchange between cells. Nat Cell Biol 2007;9:654-659.
38 Keller S, Ridinger J, Rupp AK, Janssen JW, Altevogt P: Body fluid derived exosomes as a novel template for clinical diagnostics. J Transl Med 2011;9:86.
39 Cappello F, Logozzi M, Campanella C, Bavisotto CC, Marcilla A, Properzi F, Fais S: Exosome levels in human body fluids: A tumor marker by themselves? Eur J Pharm Sci 2017;96:93-98.
40 Gallo A, Tandon M, Alevizos I, Illei GG: The majority of microrna detectable in serum and saliva is concentrated in exosomes. PLoS One 2012;7:e30679.
41 Koga Y, Yasunaga M, Moriya Y, Akasu T, Fujita S, Yamamoto S, Matsumura Y: Exosome can prevent rnase from degrading microrna in feces. J Gastrointest Oncol 2011;2:215-222.
42 Liao Y, Du X, Li J, Lonnerdal B: Human milk exosomes and their micrornas survive digestion in vitro and are taken up by human intestinal cells. Mol Nutr Food Res 2017
43 Azmi AS, Bao B, Sarkar FH: Exosomes in cancer development, metastasis, and drug resistance: A comprehensive review. Cancer Metastasis Rev 2013;32:623-642.
44 Milane L, Singh A, Mattheolabakis G, Suresh M, Amiji MM: Exosome mediated communication within the tumor microenvironment. J Control Release 2015;219:278-294.
45 Frydrychowicz M, Kolecka-Bednarczyk A, Madejczyk M, Yasar S, Dworacki G: Exosomes - structure, biogenesis and biological role in non-small-cell lung cancer. Scand J Immunol 2015;81:2-10.

46 Raposo G, Stoorvogel W: Extracellular vesicles: Exosomes, microvesicles, and friends. J Cell Biol 2013;200:373-383.
47 Bobrie A, Colombo M, Raposo G, Thery C: Exosome secretion: Molecular mechanisms and roles in immune responses. Traffic 2011;12:1659-1668.
48 Subra C, Grand D, Laulagnier K, Stella A, Lambeau G, Paillasse M, De Medina P, Monsarrat B, Perret B, Silvente-Poirot S, Poirot M, Record M: Exosomes account for vesicle-mediated transcellular transport of activatable phospholipases and prostaglandins. J Lipid Res 2010;51:2105-2120.
49 Hannafon BN, Ding WQ: Intercellular communication by exosome-derived micrornas in cancer. Int J Mol Sci 2013;14:14240-14269.
50 Andreu Z, Yanez-Mo M: Tetraspanins in extracellular vesicle formation and function. Front Immunol 2014;5:442.
51 Mazurov D, Barbashova L, Filatov A: Tetraspanin protein cd9 interacts with metalloprotease cd10 and enhances its release via exosomes. FEBS J 2013;280:1200-1213.
52 Vlassov AV, Magdaleno S, Setterquist R, Conrad R: Exosomes: Current knowledge of their composition, biological functions, and diagnostic and therapeutic potentials. Biochim Biophys Acta 2012;1820:940-948.
53 Gross JC, Chaudhary V, Bartscherer K, Boutros M: Active wnt proteins are secreted on exosomes. Nat Cell Biol 2012;14:1036-1045.
54 Sheldon H, Heikamp E, Turley H, Dragovic R, Thomas P, Oon CE, Leek R, Edelmann M, Kessler B, Sainson RC, Sargent I, Li JL, Harris AL: New mechanism for notch signaling to endothelium at a distance by delta-like 4 incorporation into exosomes. Blood 2010;116:2385-2394.
55 Erb U, Zoller M: Progress and potential of exosome analysis for early pancreatic cancer detection. Expert Rev Mol Diagn 2016;16:757-767.
56 Colombo M, Raposo G, Thery C: Biogenesis, secretion, and intercellular interactions of exosomes and other extracellular vesicles. Annu Rev Cell Dev Biol 2014;30:255-289.
57 Lund E, Guttinger S, Calado A, Dahlberg JE, Kutay U: Nuclear export of microrna precursors. Science 2004;303:95-98.
58 Zhang J, Li S, Li L, Li M, Guo C, Yao J, Mi S: Exosome and exosomal microrna: Trafficking, sorting, and function. Genomics Proteomics Bioinformatics 2015;13:17-24.
59 Guescini M, Guidolin D, Vallorani L, Casadei L, Gioacchini AM, Tibollo P, Battistelli M, Falcieri E, Battistin L, Agnati LF, Stocchi V: C2c12 myoblasts release micro-vesicles containing mtdna and proteins involved in signal transduction. Exp Cell Res 2010;316:1977-1984.
60 Balaj L, Lessard R, Dai L, Cho YJ, Pomeroy SL, Breakefield XO, Skog J: Tumour microvesicles contain retrotransposon elements and amplified oncogene sequences. Nat Commun 2011;2:180.
61 Kahlert C, Melo SA, Protopopov A, Tang J, Seth S, Koch M, Zhang J, Weitz J, Chin L, Futreal A, Kalluri R: Identification of double-stranded genomic DNA spanning all chromosomes with mutated kras and p53 DNA in the serum exosomes of patients with pancreatic cancer. J Biol Chem 2014;289:3869-3875.
62 Kalluri R, LeBleu VS: Discovery of double-stranded genomic DNA in circulating exosomes. Cold Spring Harb Symp Quant Biol 2016;81:275-280.
63 Sun Y, Liu J: Potential of cancer cell-derived exosomes in clinical application: A review of recent research advances. Clin Ther 2014;36:863-872.
64 Ribeiro MF, Zhu H, Millard RW, Fan GC: Exosomes function in pro- and anti-angiogenesis. Curr Angiogenes 2013;2:54-59.
65 Mineo M, Garfield SH, Taverna S, Flugy A, De Leo G, Alessandro R, Kohn EC: Exosomes released by k562 chronic myeloid leukemia cells promote angiogenesis in a src-dependent fashion. Angiogenesis 2012;15:33-45.
66 Kucharzewska P, Christianson HC, Welch JE, Svensson KJ, Fredlund E, Ringner M, Morgelin M, Bourseau-Guilmain E, Bengzon J, Belting M: Exosomes reflect the hypoxic status

of glioma cells and mediate hypoxia-dependent activation of vascular cells during tumor development. Proc Natl Acad Sci U S A 2013;110:7312-7317.
67 Momen-Heravi F: Isolation of extracellular vesicles by ultracentrifugation. Methods Mol Biol 2017;1660:25-32.
68 Peterson MF, Otoc N, Sethi JK, Gupta A, Antes TJ: Integrated systems for exosome investigation. Methods 2015;87:31-45.
69 Zarovni N, Corrado A, Guazzi P, Zocco D, Lari E, Radano G, Muhhina J, Fondelli C, Gavrilova J, Chiesi A: Integrated isolation and quantitative analysis of exosome shuttled proteins and nucleic acids using immunocapture approaches. Methods 2015;87:46-58.
70 Pospichalova V, Svoboda J, Dave Z, Kotrbova A, Kaiser K, Klemova D, Ilkovics L, Hampl A, Crha I, Jandakova E, Minar L, Weinberger V, Bryja V: Simplified protocol for flow cytometry analysis of fluorescently labeled exosomes and microvesicles using dedicated flow cytometer. J Extracell Vesicles 2015;4:25530.
71 Logozzi M, De Milito A, Lugini L, Borghi M, Calabro L, Spada M, Perdicchio M, Marino ML, Federici C, Iessi E, Brambilla D, Venturi G, Lozupone F, Santinami M, Huber V, Maio M, Rivoltini L, Fais S: High levels of exosomes expressing cd63 and caveolin-1 in plasma of melanoma patients. PLoS One 2009;4:e5219.
72 Madhavan B, Yue S, Galli U, Rana S, Gross W, Muller M, Giese NA, Kalthoff H, Becker T, Buchler MW, Zoller M: Combined evaluation of a panel of protein and mirna serum-exosome biomarkers for pancreatic cancer diagnosis increases sensitivity and specificity. Int J Cancer 2015;136:2616-2627.
73 Wang H, Rana S, Giese N, Buchler MW, Zoller M: Tspan8, cd44v6 and alpha6beta4 are biomarkers of migrating pancreatic cancer-initiating cells. Int J Cancer 2013;133:416-426.
74 Heiler S, Wang Z, Zoller M: Pancreatic cancer stem cell markers and exosomes - the incentive push. World J Gastroenterol 2016;22:5971-6007.
75 Darwish IA, Al-Obaid AR, Al-Malaq HA: Validated enzyme-linked immunosorbent assay for determination of rosuvastatin in plasma at picogram level. Drug Test Anal 2013;5:334-339.
76 Bosteen MH, Dahlback B, Nielsen LB, Christoffersen C: Protein unfolding allows use of commercial antibodies in an apolipoprotein m sandwich elisa. J Lipid Res 2015;56:754-759.
77 Kumar A, Pulicherla KK, Sambasiva Rao KR: Development and validation of an indirect competitive elisa for quantification of recombinant staphylokinase in rabbit plasma: Application to pharmacokinetic study. J Immunoassay Immunochem 2016;37:228-242.
78 Berth M, Bosmans E: Prevention of assay interference in infectious-disease serology tests done on the liaison platform. Clin Vaccine Immunol 2008;15:891-892.
79 Haycock JW: Polyvinylpyrrolidone as a blocking agent in immunochemical studies. Anal Biochem 1993;208:397-399.
80 Moroncini G, Grieco A, Nacci G, Paolini C, Tonnini C, Pozniak KN, Cuccioloni M, Mozzicafreddo M, Svegliati S, Angeletti M, Kazlauskas A, Avvedimento EV, Funaro A, Gabrielli A: Epitope specificity determines pathogenicity and detectability of anti-platelet-derived growth factor receptor alpha autoantibodies in systemic sclerosis. Arthritis Rheumatol 2015;67:1891-1903.
81 O'Toole M, Legault H, Ramsey R, Wynn TA, Kasaian MT: A novel and sensitive elisa reveals that the soluble form of il-13r-alpha2 is not expressed in plasma of healthy or asthmatic subjects. Clin Exp Allergy 2008;38:594-601.
82 Bandari SK, Purushothaman A, Ramani VC, Brinkley GJ, Chandrashekar DS, Varambally S, Mobley JA, Zhang Y, Brown EE, Vlodavsky I, Sanderson RD: Chemotherapy induces secretion of exosomes loaded with heparanase that degrades extracellular matrix and impacts tumor and host cell behavior. Matrix Biol 2017
83 Li W, Li C, Zhou T, Liu X, Li X, Chen D: Role of exosomal proteins in cancer diagnosis. Mol Cancer 2017;16:145.

84 Runz S, Keller S, Rupp C, Stoeck A, Issa Y, Koensgen D, Mustea A, Sehouli J, Kristiansen G, Altevogt P: Malignant ascites-derived exosomes of ovarian carcinoma patients contain cd24 and epcam. Gynecol Oncol 2007;107:563-571.
85 Bachet JB, Marechal R, Demetter P, Bonnetain F, Couvelard A, Svrcek M, Bardier-Dupas A, Hammel P, Sauvanet A, Louvet C, Paye F, Rougier P, Penna C, Vaillant JC, Andre T, Closset J, Salmon I, Emile JF, Van Laethem JL: Contribution of cxcr4 and smad4 in predicting disease progression pattern and benefit from adjuvant chemotherapy in resected pancreatic adenocarcinoma. Ann Oncol 2012;23:2327-2335.
86 Marechal R, Demetter P, Nagy N, Berton A, Decaestecker C, Polus M, Closset J, Deviere J, Salmon I, Van Laethem JL: High expression of cxcr4 may predict poor survival in resected pancreatic adenocarcinoma. Br J Cancer 2009;100:1444-1451.
87 Wu H, Zhu L, Zhang H, Shi X, Zhang L, Wang W, Xue H, Liang Z: Coexpression of egfr and cxcr4 predicts poor prognosis in resected pancreatic ductal adenocarcinoma. PLoS One 2015;10:e0116803.
88 Krieg A, Riemer JC, Telan LA, Gabbert HE, Knoefel WT: Cxcr4--a prognostic and clinicopathological biomarker for pancreatic ductal adenocarcinoma: A meta-analysis. PLoS One 2015;10:e0130192.
89 Dalla Pozza E, Dando I, Biondani G, Brandi J, Costanzo C, Zoratti E, Fassan M, Boschi F, Melisi D, Cecconi D, Scupoli MT, Scarpa A, Palmieri M: Pancreatic ductal adenocarcinoma cell lines display a plastic ability to bidirectionally convert into cancer stem cells. Int J Oncol 2015;46:1099-1108.
90 Castillo J, Bernard V, San Lucas FA, Allenson K, Capello M, Kim DU, Gascoyne P, Mulu FC, Stephens BM, Huang J, Wang H, Momin AA, Jacamo RO, Katz M, Wolff R, Javle M, Varadhachary G, Wistuba, II, Hanash S, Maitra A, Alvarez H: Surfaceome profiling enables isolation of cancer-specific exosomal cargo in liquid biopsies from pancreatic cancer patients. Ann Oncol 2017
91 Nazarenko I, Rana S, Baumann A, McAlear J, Hellwig A, Trendelenburg M, Lochnit G, Preissner KT, Zoller M: Cell surface tetraspanin tspan8 contributes to molecular pathways of exosome-induced endothelial cell activation. Cancer Res 2010;70:1668-1678.
92 Zhao W, Langfelder P, Fuller T, Dong J, Li A, Hovarth S: Weighted gene coexpression network analysis: State of the art. J Biopharm Stat 2010;20:281-300.
93 Stuart JM, Segal E, Koller D, Kim SK: A gene-coexpression network for global discovery of conserved genetic modules. Science 2003;302:249-255.
94 Zhang B, Horvath S: A general framework for weighted gene co-expression network analysis. Stat Appl Genet Mol Biol 2005;4:Article17.
95 Yu X, Feng L, Liu D, Zhang L, Wu B, Jiang W, Han Z, Cheng S: Quantitative proteomics reveals the novel co-expression signatures in early brain development for prognosis of glioblastoma multiforme. Oncotarget 2016;7:14161-14171.
96 Jia X, Miao Z, Li W, Zhang L, Feng C, He Y, Bi X, Wang L, Du Y, Hou M, Hao D, Xiao Y, Chen L, Li K: Cancer-risk module identification and module-based disease risk evaluation: A case study on lung cancer. PLoS One 2014;9:e92395.
97 Clarke C, Madden SF, Doolan P, Aherne ST, Joyce H, O'Driscoll L, Gallagher WM, Hennessy BT, Moriarty M, Crown J, Kennedy S, Clynes M: Correlating transcriptional networks to breast cancer survival: A large-scale coexpression analysis. Carcinogenesis 2013;34:2300-2308.
98 Frampton AE, Castellano L, Colombo T, Giovannetti E, Krell J, Jacob J, Pellegrino L, Roca-Alonso L, Funel N, Gall TM, De Giorgio A, Pinho FG, Fulci V, Britton DJ, Ahmad R, Habib NA, Coombes RC, Harding V, Knosel T, Stebbing J, Jiao LR: Microrna cooperatively inhibit a network of tumor suppressor genes to promote pancreatic tumor growth and progression. Gastroenterology 2014;146:268-277 e218.
99 Kojima M, Sudo H, Kawauchi J, Takizawa S, Kondou S, Nobumasa H, Ochiai A: Microrna markers for the diagnosis of pancreatic and biliary-tract cancers. PLoS One 2015;10:e0118220.

100 Irizarry RA, Hobbs B, Collin F, Beazer-Barclay YD, Antonellis KJ, Scherf U, Speed TP: Exploration, normalization, and summaries of high density oligonucleotide array probe level data. Biostatistics 2003;4:249-264.
101 Langfelder P, Horvath S: Wgcna: An r package for weighted correlation network analysis. BMC Bioinformatics 2008;9:559.
102 Miller JA, Cai C, Langfelder P, Geschwind DH, Kurian SM, Salomon DR, Horvath S: Strategies for aggregating gene expression data: The collapserows r function. BMC Bioinformatics 2011;12:322.
103 Johnson WE, Li C, Rabinovic A: Adjusting batch effects in microarray expression data using empirical bayes methods. Biostatistics 2007;8:118-127.
104 Chen C, Grennan K, Badner J, Zhang D, Gershon E, Jin L, Liu C: Removing batch effects in analysis of expression microarray data: An evaluation of six batch adjustment methods. PLoS One 2011;6:e17238.
105 Oldham MC, Langfelder P, Horvath S: Network methods for describing sample relationships in genomic datasets: Application to huntington's disease. BMC Syst Biol 2012;6:63.
106 Langfelder P, Luo R, Oldham MC, Horvath S: Is my network module preserved and reproducible? PLoS Comput Biol 2011;7:e1001057.
107 Horvath S, Dong J: Geometric interpretation of gene coexpression network analysis. PLoS Comput Biol 2008;4:e1000117.
108 Huang DW, Sherman BT, Tan Q, Kir J, Liu D, Bryant D, Guo Y, Stephens R, Baseler MW, Lane HC, Lempicki RA: David bioinformatics resources: Expanded annotation database and novel algorithms to better extract biology from large gene lists. Nucleic Acids Res 2007;35:W169-175.
109 Chen EY, Tan CM, Kou Y, Duan Q, Wang Z, Meirelles GV, Clark NR, Ma'ayan A: Enrichr: Interactive and collaborative html5 gene list enrichment analysis tool. BMC Bioinformatics 2013;14:128.
110 Fan Y, Siklenka K, Arora SK, Ribeiro P, Kimmins S, Xia J: Mirnet - dissecting mirna-target interactions and functional associations through network-based visual analysis. Nucleic Acids Res 2016;44:W135-141.
111 Aguirre-Gamboa R, Gomez-Rueda H, Martinez-Ledesma E, Martinez-Torteya A, Chacolla-Huaringa R, Rodriguez-Barrientos A, Tamez-Pena JG, Trevino V: Survexpress: An online biomarker validation tool and database for cancer gene expression data using survival analysis. PLoS One 2013;8:e74250.
112 Aguirre-Gamboa R, Trevino V: Survmicro: Assessment of mirna-based prognostic signatures for cancer clinical outcomes by multivariate survival analysis. Bioinformatics 2014;30:1630-1632.
113 Carlson MR, Zhang B, Fang Z, Mischel PS, Horvath S, Nelson SF: Gene connectivity, function, and sequence conservation: Predictions from modular yeast co-expression networks. BMC Genomics 2006;7:40.
114 Miller JA, Horvath S, Geschwind DH: Divergence of human and mouse brain transcriptome highlights alzheimer disease pathways. Proc Natl Acad Sci U S A 2010;107:12698-12703.
115 Oldham MC, Konopka G, Iwamoto K, Langfelder P, Kato T, Horvath S, Geschwind DH: Functional organization of the transcriptome in human brain. Nat Neurosci 2008;11:1271-1282.
116 Buchholz M, Braun M, Heidenblut A, Kestler HA, Kloppel G, Schmiegel W, Hahn SA, Luttges J, Gress TM: Transcriptome analysis of microdissected pancreatic intraepithelial neoplastic lesions. Oncogene 2005;24:6626-6636.
117 Jeong W, Lee DY, Park S, Rhee SG: Erp16, an endoplasmic reticulum-resident thiol-disulfide oxidoreductase: Biochemical properties and role in apoptosis induced by endoplasmic reticulum stress. J Biol Chem 2008;283:25557-25566.

118 Raturi A, Simmen T: Where the endoplasmic reticulum and the mitochondrion tie the knot: The mitochondria-associated membrane (mam). Biochim Biophys Acta 2013;1833:213-224.
119 Kuo KK, Kuo CJ, Chiu CY, Liang SS, Huang CH, Chi SW, Tsai KB, Chen CY, Hsi E, Cheng KH, Chiou SH: Quantitative proteomic analysis of differentially expressed protein profiles involved in pancreatic ductal adenocarcinoma. Pancreas 2016;45:71-83.
120 Nakamura T, Furukawa Y, Nakagawa H, Tsunoda T, Ohigashi H, Murata K, Ishikawa O, Ohgaki K, Kashimura N, Miyamoto M, Hirano S, Kondo S, Katoh H, Nakamura Y, Katagiri T: Genome-wide cdna microarray analysis of gene expression profiles in pancreatic cancers using populations of tumor cells and normal ductal epithelial cells selected for purity by laser microdissection. Oncogene 2004;23:2385-2400.
121 Dawelbait G, Winter C, Zhang Y, Pilarsky C, Grutzmann R, Heinrich JC, Schroeder M: Structural templates predict novel protein interactions and targets from pancreas tumour gene expression data. Bioinformatics 2007;23:i115-124.
122 Nussinov R, Muratcioglu S, Tsai CJ, Jang H, Gursoy A, Keskin O: The key role of calmodulin in kras-driven adenocarcinomas. Mol Cancer Res 2015;13:1265-1273.
123 Dong Q, Zhang Y, Yang XH, Jing W, Zheng LQ, Liu YP, Qu XJ, Li Z: Serum calcium level used as a prognostic predictor in patients with resectable pancreatic ductal adenocarcinoma. Clin Res Hepatol Gastroenterol 2014;38:639-648.
124 Swierczynski J, Hebanowska A, Sledzinski T: Role of abnormal lipid metabolism in development, progression, diagnosis and therapy of pancreatic cancer. World J Gastroenterol 2014;20:2279-2303.
125 Simeone DM, Ji B, Banerjee M, Arumugam T, Li D, Anderson MA, Bamberger AM, Greenson J, Brand RE, Ramachandran V, Logsdon CD: Ceacam1, a novel serum biomarker for pancreatic cancer. Pancreas 2007;34:436-443.
126 Kalinina T, Gungor C, Thieltges S, Moller-Krull M, Penas EM, Wicklein D, Streichert T, Schumacher U, Kalinin V, Simon R, Otto B, Dierlamm J, Schwarzenbach H, Effenberger KE, Bockhorn M, Izbicki JR, Yekebas EF: Establishment and characterization of a new human pancreatic adenocarcinoma cell line with high metastatic potential to the lung. BMC Cancer 2010;10:295.
127 Gebauer F, Wicklein D, Horst J, Sundermann P, Maar H, Streichert T, Tachezy M, Izbicki JR, Bockhorn M, Schumacher U: Carcinoembryonic antigen-related cell adhesion molecules (ceacam) 1, 5 and 6 as biomarkers in pancreatic cancer. PLoS One 2014;9:e113023.
128 Farhana L, Dawson MI, Fontana JA: Down regulation of mir-202 modulates mxd1 and sin3a repressor complexes to induce apoptosis of pancreatic cancer cells. Cancer Biol Ther 2015;16:115-124.
129 Tabach Y, Kogan-Sakin I, Buganim Y, Solomon H, Goldfinger N, Hovland R, Ke XS, Oyan AM, Kalland KH, Rotter V, Domany E: Amplification of the 20q chromosomal arm occurs early in tumorigenic transformation and may initiate cancer. PLoS One 2011;6:e14632.
130 Liang JW, Shi ZZ, Shen TY, Che X, Wang Z, Shi SS, Xu X, Cai Y, Zhao P, Wang CF, Zhou ZX, Wang MR: Identification of genomic alterations in pancreatic cancer using array-based comparative genomic hybridization. PLoS One 2014;9:e114616.
131 Bauer AS, Keller A, Costello E, Greenhalf W, Bier M, Borries A, Beier M, Neoptolemos J, Buchler M, Werner J, Giese N, Hoheisel JD: Diagnosis of pancreatic ductal adenocarcinoma and chronic pancreatitis by measurement of microrna abundance in blood and tissue. PLoS One 2012;7:e34151.
132 Ali S, Almhanna K, Chen W, Philip PA, Sarkar FH: Differentially expressed mirnas in the plasma may provide a molecular signature for aggressive pancreatic cancer. Am J Transl Res 2010;3:28-47.
133 Lin MS, Chen WC, Huang JX, Gao HJ, Sheng HH: Aberrant expression of micrornas in serum may identify individuals with pancreatic cancer. Int J Clin Exp Med 2014;7:5226-5234.

134 Liu J, Gao J, Du Y, Li Z, Ren Y, Gu J, Wang X, Gong Y, Wang W, Kong X: Combination of plasma microrna s with serum ca19-9 for early detection of pancreatic cancer. Int J Cancer 2012;131:683-691.
135 Wang J, Chen J, Chang P, LeBlanc A, Li D, Abbruzzesse JL, Frazier ML, Killary AM, Sen S: Micrornas in plasma of pancreatic ductal adenocarcinoma patients as novel blood-based biomarkers of disease. Cancer Prev Res (Phila) 2009;2:807-813.
136 Nunes LM, Robles-Escajeda E, Santiago-Vazquez Y, Ortega NM, Lema C, Muro A, Almodovar G, Das U, Das S, Dimmock JR, Aguilera RJ, Varela-Ramirez A: The gender of cell lines matters when screening for novel anti-cancer drugs. AAPS J 2014;16:872-874.
137 Ali R, Barnes I, Cairns BJ, Finlayson AE, Bhala N, Mallath M, Beral V: Incidence of gastrointestinal cancers by ethnic group in england, 2001-2007. Gut 2013;62:1692-1703.
138 Singal V, Singal AK, Kuo YF: Racial disparities in treatment for pancreatic cancer and impact on survival: A population-based analysis. J Cancer Res Clin Oncol 2012;138:715-722.
139 Herr I, Lozanovski V, Houben P, Schemmer P, Buchler MW: Sulforaphane and related mustard oils in focus of cancer prevention and therapy. Wien Med Wochenschr 2013;163:80-88.
140 Larsson SC, Hakansson N, Naslund I, Bergkvist L, Wolk A: Fruit and vegetable consumption in relation to pancreatic cancer risk: A prospective study. Cancer Epidemiol Biomarkers Prev 2006;15:301-305.
141 Kirsh VA, Peters U, Mayne ST, Subar AF, Chatterjee N, Johnson CC, Hayes RB: Prospective study of fruit and vegetable intake and risk of prostate cancer. J Natl Cancer Inst 2007;99:1200-1209.
142 Kallifatidis G, Rausch V, Baumann B, Apel A, Beckermann BM, Groth A, Mattern J, Li Z, Kolb A, Moldenhauer G, Altevogt P, Wirth T, Werner J, Schemmer P, Büchler MW, Salnikov A, Herr I: Sulforaphane targets pancreatic tumour-initiating cells by nf-kappab-induced antiapoptotic signalling. Gut 2009;58:949-963.
143 Kallifatidis G, Labsch S, Rausch V, Mattern J, Gladkich J, Moldenhauer G, Büchler MW, Salnikov A, Herr I: Sulforaphane increases drug-mediated cytotoxicity towards cancer stem-like cells of pancreas and prostate. Mol Ther 2011;19:188-195.
144 Taylor RC, Cullen SP, Martin SJ: Apoptosis: Controlled demolition at the cellular level. Nature Reviews: Molecular Cell Biology 2008;9:231-241.
145 Su Z, Yang Z, Xie L, DeWitt JP, Chen Y: Cancer therapy in the necroptosis era. Cell Death Differ 2016;23:748-756.
146 Vandenabeele P, Galluzzi L, Vanden Berghe T, Kroemer G: Molecular mechanisms of necroptosis: An ordered cellular explosion. Nat Rev Mol Cell Biol 2010;11:700-714.
147 Sun L, Wang H, Wang Z, He S, Chen S, Liao D, Wang L, Yan J, Liu W, Lei X, Wang X: Mixed lineage kinase domain-like protein mediates necrosis signaling downstream of rip3 kinase. Cell 2012;148:213-227.
148 Weinlich R, Oberst A, Beere HM, Green DR: Necroptosis in development, inflammation and disease. Nat Rev Mol Cell Biol 2017;18:127-136.
149 Dondelinger Y, Jouan-Lanhouet S, Divert T, Theatre E, Bertin J, Gough PJ, Giansanti P, Heck AJ, Dejardin E, Vandenabeele P, Bertrand MJ: Nf-kappab-independent role of ikkalpha/ikkbeta in preventing ripk1 kinase-dependent apoptotic and necroptotic cell death during tnf signaling. Mol Cell 2015;60:63-76.
150 Wu YT, Tan HL, Huang Q, Sun XJ, Zhu X, Shen HM: Zvad-induced necroptosis in l929 cells depends on autocrine production of tnfalpha mediated by the pkc-mapks-ap-1 pathway. Cell Death Differ 2011;18:26-37.
151 Fan P, Zhang Y, Liu L, Zhao Z, Yin Y, Xiao X, Bauer N, Gladkich J, Mattern J, Gao C, Schemmer P, Gross W, Herr I: Continuous exposure of pancreatic cancer cells to dietary bioactive agents does not induce drug resistance unlike chemotherapy. Cell Death Dis 2016;7:e2246.

152 Heller A, Angelova AL, Bauer S, Grekova SP, Aprahamian M, Rommelaere J, Volkmar M, Janssen JW, Bauer N, Herr I, Giese T, Gaida MM, Bergmann F, Hackert T, Fritz S, Giese NA: Establishment and characterization of a novel cell line, asan-paca, derived from human adenocarcinoma arising in intraductal papillary mucinous neoplasm of the pancreas. Pancreas 2016;45:1452-1460.
153 Zhang Y, Liu L, Fan P, Bauer N, Gladkich J, Ryschich E, Bazhin AV, Giese NA, Strobel O, Hackert T, Hinz U, Gross W, Fortunato F, Herr I: Aspirin counteracts cancer stem cell features, desmoplasia and gemcitabine resistance in pancreatic cancer. Oncotarget 2015;6:9999-10015.
154 Degterev A, Hitomi J, Germscheid M, Ch'en IL, Korkina O, Teng X, Abbott D, Cuny GD, Yuan C, Wagner G, Hedrick SM, Gerber SA, Lugovskoy A, Yuan J: Identification of rip1 kinase as a specific cellular target of necrostatins. Nat Chem Biol 2008;4:313-321.
155 Vandenabeele P, Grootjans S, Callewaert N, Takahashi N: Necrostatin-1 blocks both ripk1 and ido: Consequences for the study of cell death in experimental disease models. Cell Death Differ 2013;20:185-187.
156 Degterev A, Zhou W, Maki JL, Yuan J: Assays for necroptosis and activity of rip kinases. Methods Enzymol 2014;545:1-33.
157 McComb S, Shutinoski B, Thurston S, Cessford E, Kumar K, Sad S: Cathepsins limit macrophage necroptosis through cleavage of rip1 kinase. J Immunol 2014;192:5671-5678.
158 McComb S, Cheung HH, Korneluk RG, Wang S, Krishnan L, Sad S: Ciap1 and ciap2 limit macrophage necroptosis by inhibiting rip1 and rip3 activation. Cell Death Differ 2012;19:1791-1801.
159 Kallifatidis G, Rausch V, Baumann B, Apel A, Beckermann BM, Groth A, Mattern J, Li Z, Kolb A, Moldenhauer G, Altevogt P, Wirth T, Werner J, Schemmer P, Buchler MW, Salnikov AV, Herr I: Sulforaphane targets pancreatic tumour-initiating cells by nf-kappab-induced antiapoptotic signalling. Gut 2009;58:949-963.
160 Kallifatidis G, Labsch S, Rausch V, Mattern J, Gladkich J, Moldenhauer G, Buchler MW, Salnikov AV, Herr I: Sulforaphane increases drug-mediated cytotoxicity toward cancer stem-like cells of pancreas and prostate. Mol Ther 2011;19:188-195.
161 Rausch V, Liu L, Kallifatidis G, Baumann B, Mattern J, Gladkich J, Wirth T, Schemmer P, Buchler MW, Zoller M, Salnikov AV, Herr I: Synergistic activity of sorafenib and sulforaphane abolishes pancreatic cancer stem cell characteristics. Cancer Res 2010;70:5004-5013.
162 Rackauskas R, Zhou D, Uselis S, Strupas K, Herr I, Schemmer P: Sulforaphane sensitizes human cholangiocarcinoma to cisplatin via the downregulation of anti-apoptotic proteins. Oncol Rep 2017;37:3660-3666.
163 Oliver Metzig M, Fuchs D, Tagscherer KE, Grone HJ, Schirmacher P, Roth W: Inhibition of caspases primes colon cancer cells for 5-fluorouracil-induced tnf-alpha-dependent necroptosis driven by rip1 kinase and nf-kappab. Oncogene 2016;35:3399-3409.
164 Hannes S, Abhari BA, Fulda S: Smac mimetic triggers necroptosis in pancreatic carcinoma cells when caspase activation is blocked. Cancer Lett 2016;380:31-38.
165 Dunai ZA, Imre G, Barna G, Korcsmaros T, Petak I, Bauer PI, Mihalik R: Staurosporine induces necroptotic cell death under caspase-compromised conditions in u937 cells. PLoS One 2012;7:e41945.